AD NUMBER

AD801619

NEW LIMITATION CHANGE

TO

Approved for public release, distribution unlimited

FROM

Distribution authorized to U.S. Gov't. agencies and their contractors; Critical Technology; MAY 1966. Other requests shall be referred to Air Force Space Systems Division, Attn: SMC-HO, Los Angeles AFB, CA.

AUTHORITY

samso ltr, 24 jan 1972

AEROSPACE REPORT NO.
TR-669(2240-20)-7

# Electron Collision Cross Sections in Air and the Effects of Elevated Gas Temperatures

JULY 1966

*Prepared by* CARL J. LENANDER
*Aerodynamics and Propulsion Research Laboratory*
*Laboratories Division*
*Laboratory Operations*
AEROSPACE CORPORATION

*Prepared for* BALLISTIC SYSTEMS AND SPACE SYSTEMS DIVISIONS
AIR FORCE SYSTEMS COMMAND
LOS ANGELES AIR FORCE STATION
*Los Angeles, California*

AIR FORCE REPORT NO.
SSD-TR-66-153

AEROSPACE REPORT NO.
TR-669(6240-20)-7

# ELECTRON COLLISION CROSS SECTIONS IN AIR AND THE EFFECTS OF ELEVATED GAS TEMPERATURES


Prepared by

Carl J. Lenander
Aerodynamics and Propulsion Research Laboratory

Laboratories Division
Laboratory Operations
AEROSPACE CORPORATION



May 1966


Prepared for

BALLISTIC SYSTEMS AND SPACE SYSTEMS DIVISIONS
AIR FORCE SYSTEMS COMMAND
LOS ANGELES AIR FORCE STATION
Los Angeles, California

## FOREWORD

This report is published by Aerospace Corporation, El Segundo, California, under Air Force Contract No. AF 04(695)-669.

This report, which documents research conducted between June 1965 and June 1966, was submitted on 15 August 1966 to Captain Ronald J. Starbuck, SSTRT, for review and approval.

Information in this report is embargoed under the U. S. Export Control Act of 1949, administered by the Department of Commerce. This report may be released by departments or agencies of the U. S. Government to departments or agencies of foreign governments with which the United States has defense treaty commitments. Private individuals or firms must comply with Department of Commerce export control regulations.

The author wishes to express his appreciation to all the publications from which the figures were extracted. Permission to use each figure has been granted. The sources are credited at the end of each caption.

Approved

J. G. Logan, Director
Aerodynamics and Propulsion
Research Laboratory

Publication of this report does not constitute Air Force approval of the report's findings or conclusions. It is published only for the exchange and stimulation of ideas.

Ronald J. Starbuck
Captain, USAF

## ABSTRACT

Elastic and inelastic electron scattering cross sections in air or its constituent gases are normally studied at low gas temperatures, therefore the initial state of the scatterer is the ground state. However, in the study of transport phenomena in gases, such as the propagation of intense electromagnetic waves through a reentry flow field where the gas temperature may easily reach a value on the order of 6,000°K and the electron temperature may be many times that value, it is necessary to include the effect of the scatterers being distributed in excited states as well as in the ground state. For the temperatures of interest, the states populated will be rotational and vibrational, with virtually no effect from excited electronic levels because they lie too high in energy above the ground state. The species considered are N, O, A, $N_2$, $O_2$, and NO and some of their ions. This report is intended as a catalogue of the best available cross sections for the various processes and is presented in a manner to be useful as an aid in transport phenomena calculations.

CONTENTS

## FIGURES

FIGURES (Continued)

## TABLES

# I. INTRODUCTION

This report is an outgrowth of the study of propagation of high intensity electromagnetic waves in air under reentry conditions. In this study it was necessary to examine all of the possible electron collision mechanisms for the principal constituents of air. It was found that there was no single, up-to-date collection of this material, and many of the existing sources presented material in a form that was not readily usable by a large group of people interested in certain transport phenomena. Further, the subject of temperature-dependent cross sections for gas, which is recently increasing in popularity, is not treated in the usual available compenda. The intention of this report is to present the best available cross sections, including recently published results, in a usable catalogue form and to provide, where applicable, a discussion of temperature dependence. The style of presentation is intended to be purely expository. The cross sections are presented in separate sections concerned with particular scattering processes, and no importance is implied by the selected order of sections. A summary is provided at the end of each section to demonstrate a comparative evaluation for the species considered.

## II. TEMPERATURE DEPENDENT CROSS SECTIONS

The temperature dependent cross section (CS) for a given transition is given, as discussed in the Appendix, by

$$\sigma(E,T) = \frac{1}{P(T)}\left[\sigma_o(E) + \sum_{n\geq 1} \sigma_n(E) g_n \exp - \frac{\Delta E_n}{kT}\right] \qquad (1)$$

where E is the collision energy, T the temperature, P the partition function, $\sigma_o(E)$ the CS for the transition from the ground state, $\sigma_n(E)$ the CS for the transition from the nth excited state lying $\Delta E_n$ in energy above the ground state with degeneracy $g_n$, and k is Boltzmann's constant.

Population of the excited electronic states will be negligible at the temperatures of interest because the $\Delta E_n$ of Eq. (1) will be much larger (Ref. 1) than kT. Further, there is no reason for the $\sigma_n(E)$ to be large enough to balance the Boltzmann factor and be as effective as the lower lying vibrationally and rotationally excited states. Although the rotationally excited states are more numerously populated than the vibrationally excited states, in the approximation of the separation of the two motions, the effects of the latter's influence are seen to be the most important. For some of the CS, there are limits of validity on the energy range. The limit of greatest general importance is the lower energy cutoff, which is an energy where the electron begins to interact with the gas as a whole, not with the individual particles. This is arbitrarily defined as the density condition where the electron's wavelength is twice the interparticle separation. This is given by an energy $E(eV) = 2.76 \times 10^{-16} n_o^{2/3}$, where $n_o$ is the particle density per $cm^3$. This energy is referred to as $E_{n_o}$, and it can be seen to be independent of the gas temperature for a given gas density.

## III. ROTATIONAL EXCITATION

Rotational excitation and de-excitation proceeds by different interactions for homonuclear and heteronuclear diatomic molecules. For the homonuclear molecule, the permanent quadrupole field dominates the rotational scattering, and the selection rules for quadrupole interaction limit the transitions to being from an initial angular momentum state J to a final state J ± 2. Heteronuclear molecules have a permanent dipole moment. This dipole field dominates the rotational scattering, and the selection rules for dipole interaction limit the transitions from an initial J state to a final J ± 1 state.

Rotaional processes for homonuclear molecules are assumed to proceed as described by the Gerjuoy-Stein theory (Ref. 2) for transition from the i (initial) rotational state to the f (final) rotational state as

$$\sigma_{if} = \frac{8\pi(Qa_o)^2}{15} \frac{k_f}{k_i} \frac{(J+2)(J+1)}{(2J+3)(2J+1)} \tag{2a}$$

where

$$\frac{k_f}{k_i} = \left[1 - \frac{B}{E_i}(4J+6)\right]^{1/2} \tag{2b}$$

for

$$i \rightarrow f = J \rightarrow J+2$$

and

$$\sigma_{if} = \frac{8\pi(Qa_o)^2}{15} \frac{k_f}{k_i} \frac{J(J+1)}{(2J-1)(2J+1)} \tag{3a}$$

where

$$\frac{k_f}{k_i} = \left[1 - \frac{B}{E_i}(4J - 2)\right]^{1/2} \tag{3b}$$

for $i \rightarrow f = J \rightarrow J - 2$. In these equations, Q is the diatomic molecule's permanent quadrupole moment in atomic units, $a_o$ is the Bohr radius, $E_i$ the incident electron's energy, B gives the rotational energy level as $J(J + 1)B$, J is the (integer) angular momentum of the initial state, and $k_i$ and $k_f$ are the electron's initial and final momenta in atomic units (1 energy unit = 13.6 eV). This theory is done in Born approximation and is for homonuclear diatomic molecules that possess a permanent electronic quadrupole moment. By the selection rules, the transitions are limited to $J \rightarrow J \pm 2$.

Gerjuoy and Stein indicate validity of their expressions to within 10 percent for $k_i^2$ and $k_f^2$ less than 0.6 eV, and the swarm experiments (Refs. 3 and 4) indicate that they are valid in $N_2$ to 1 or 2 eV, where their effect is swamped by the vibrational excitation processes. The distorted wave calculations (Refs. 5 and 6) indicate that the CS decreases rapidly at energies above 1 to 2 eV. The best approach is to use Eqs. (2a) and (3a) for electron energies less than 1 to 2 eV and to define the CS as zero for energies above that energy.

Recent calculations (Refs. 5 and 6) by the method of distorted waves with quasipolarization show that there is energy dependent structure in the CS for $E_i$ large and J small. However, swarm experiments (Refs. 3 and 4) show that the general behavior as given by the Gerjuoy-Stein theory is adequate to explain the experiment. This is probably due to two things: first, where the distorted wave theory gives a correction to the amplitude of the CS and not the energy dependence, the correction is in the opposite direction to the experimental fit (Refs. 4 and 6) and, second, the severe difference in energy dependence occurs at an energy where vibrational effects

begin to dominate (Ref. 4). In Fig. 1, $\sigma_{64}$ and $\sigma_{46}$ for $N_2$ are given as examples of Eqs. (2a) and (3a).

For a heteronuclear diatomic molecule, such as NO, that possesses a permanent electronic dipole moment, the transitions are limited to $J \rightarrow J \pm 1$ and are given by

$$\sigma_{if} = \frac{16\pi d^2}{3k_i k_f} \frac{J}{2J+1} \tag{4a}$$

for $J \rightarrow J - 1$ with

$$\Delta E_{J,J-1} = 2JB \tag{4b}$$

and

$$\sigma_{if} = \frac{16\pi d^2}{3k_i k_f} \frac{J+1}{2J+1} \tag{5a}$$

for $J \rightarrow J + 1$ with

$$\Delta E_{J,J+1} = (2J+2)B \tag{5b}$$

where $k_i = (E_i)^{1/2}$ as before, $k_f = \left(k_i^2 - \Delta E_{if}\right)^{1/2}$, J is the initial angular momentum, and d is the dipole moment. For electron energies large with respect to the rotational spacing, the CS goes as $(E_i)^{-1}$ and will be small in comparison with Eqs. (2a) and (3a) for comparable large energy. The application of the Gerjuoy-Stein criteria to Eqs. (4a) and (5a) results in uniformly valid equations at all electron energies.

To find the maximum contribution to the effective CS, the most probably occupied rotational state must be found. Differentiating the partition function for rotation (Appendix, Eq. A-7) with respect to J and solving for $J_M$

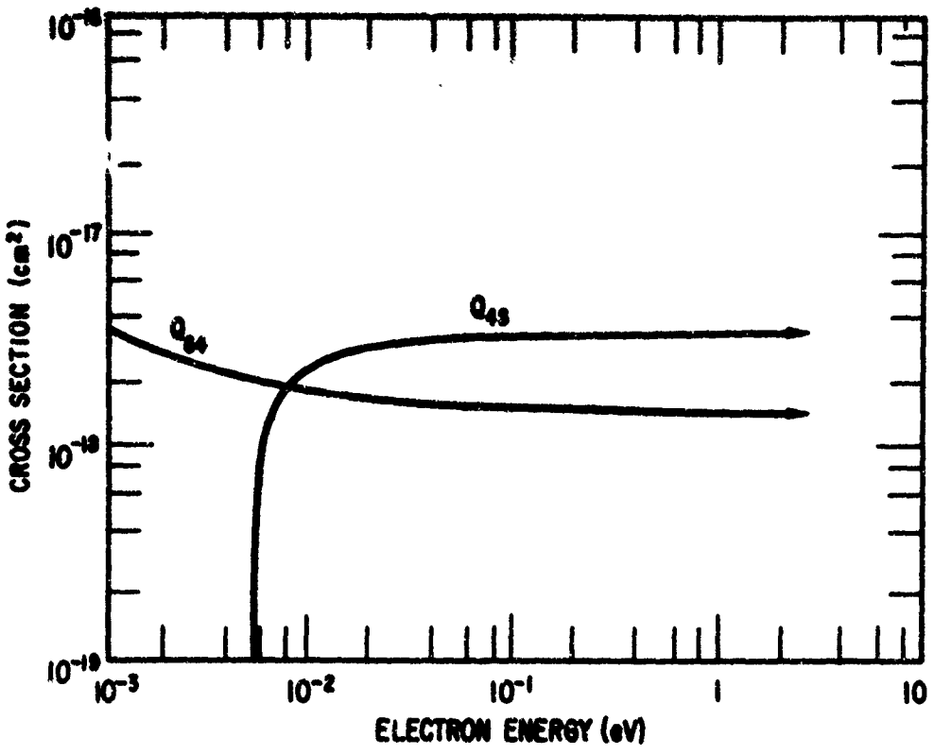


Fig. 1. Rotation Excitation CS in $N_2$ at 77°K (from Ref. 3)
$Q_{64}$ is the de-excitation CS for transition from J = 6 to J = 4, and $Q_{46}$ is the reverse transition.

gives $J_M \simeq 0.5896\,(T/B)^{1/2}$, where T is in °K and B is given in $cm^{-1}$. The probability of occupation of the Jth level is then given by $p_J = [(2J + 1)/2J_M(J_M + 1)]\ \exp[-J(J + 1)/2J_M(J_M + 1)]$. For T = 10,000°K, $J_M \simeq 41$ in $N_2$. Then using the expression for $p_J$, the maximum contribution to the effective CS (sum over J) is $(68.4)^{-1}$ times Eq. (2a) evaluated at $J_M = 41$. For J = 0, $p_J$ is $(3444)^{-1}$; thus it can be seen that the contributions from the individual levels are small. Any appreciable effect due to rotational excitation would have to come from the sum over all the J values.

Of interest in certain problems is the energy loss rate for electrons in rotational excitation collisions with molecules. If one assumes a Boltzmann distribution for the molecules, the energy loss rate is (Ref. 2)

$$\frac{dW}{dt} = \left(\frac{2E}{m}\right)^{1/2} \sum_J N_J(\sigma_{J,J+}\ \Delta E_{J,J+} - \sigma_{J,J-}\ \Delta E_{J,J-}) \tag{6}$$

where m is the electron mass, J± are J ± 1 for the dipole case and J ± 2 for the quadrupole case, and $N_J$ is the Boltzmann factor for the Jth level given by (Ref. 7) $N_J = \{(2J + 1)N \exp[-J(J + 1)B/kT]\}/P$, where N is the total number of molecules. For $E_i > 0.1$ eV, Eq. (6) can be represented satisfactorily by

$$\frac{dW}{dt} = \frac{32\pi(Qa_o)^2}{15} NB\left(\frac{2E_i}{m}\right)^{1/2} \tag{7a}$$

for the quadrupole case or

$$\frac{dW}{dt} = \frac{32\pi d^2}{3} NB\left(\frac{2}{mE_i}\right)^{1/2} \tag{7b}$$

for the dipole case, both of which are independent of temperatures.

This gives an effective energy loss coefficient[ = (1/Nv)dw/dt, v is electron velocity] for NO, $N_2$, and $O_2$ as $(1.26/E_i) \times 10^{-20}$ $5.68 \times 10^{-20}$ and $4.35 \times 10^{-20}$, respectively, where $E_i$ is in eV and the coefficient is in erg $cm^2$.

Equations (7a) and (7b) indicate that the effect of gas temperature on the rotational process is negligible. This can also be seen by putting the expressions for the CS in Eq. (1) and approximating the sum for the principal contribution due to large J, which is valid for T > 30°K. This gives an average temperature dependent CS of $4\pi(Q_{a_o})^2/15$, which is temperature independent. For $N_2$ this has the value $2.54 \times 10^{-17}$ $cm^2$.

Table 1 lists the electric moments and the rotational energy constants for the ground states of $N_2$, $O_2$, and NO for use in the appropriate CS equation.

Table 1. Dipole and Quadripole Moments and Rotational Energy Constants for $N_2$, $O_2$, and NO

| Molecule | Q, a u | d, a u | B, eV |
|---|---|---|---|
| $N_2(X^1\Sigma_g^+)$ | 1.04 | 0 | $2.49 \times 10^{-4}$ |
| $O_2(X^3\Sigma_g^-)$ | 0.796 | 0 | $1.79 \times 10^{-4}$ |
| $NO(X^2\pi)$ | -- | 0.1 | $2.12 \times 10^{-4}$ |

A summary of the rotational CS is given in Table 2.

Table 2. Rotational CS Summary

| Specie | CS | Effect of Gas Temperature | Range of Validity, eV | Remarks |
|---|---|---|---|---|
| $N_2$ | Eqs. (2a), (3a) | Independent | $En_o$ - 2 | Good agreement with experiment |
| $O_2$ | Eqs. (2a), (3a) | Independent | $En_o$ - 2 | Good agreement with experiment |
| NO | Eqs. (4a), (5a) | Independent | $En_o$ - 2 | No data available for check |

## IV. VIBRATIONAL EXCITATION

There are basically two types of vibrational excitation: direct excitation with a CS, which is nearly constant (Refs. 4 and 8) and on the order of $10^{-19}$ to $10^{-17}$ $cm^2$, and the resonance-like metastable ion formation process (Refs. 8 and 9), which has a higher structural CS on the order of $10^{-17}$ to $10^{-16}$ $cm^2$. An example of the direct excitation process for $N_2$ is shown in Fig. 2(a). The upward break in the $\sigma_{01}$ CS at 1.2 eV would not have an analog in $O_2$ and NO because they do not form metastable negative ions. The $\sigma_{10}$ CS of Fig. 1(a) was derived from $\sigma_{01}$ by detailed balancing. The vibrational excitation CS for $O_2$ is shown in Fig. 2(b). The vibrational CS for NO is unknown. Examples of these two processes occur in $N_2$ at incident electron energies between 0.3 to 1.2 eV and 1.2 to 4 eV, respectively. The resonance metastable process appears to occur only in molecules that do not form stable negative ions, such as $N_2$, and does not occur in $O_2$ and NO, which form stable negative ions. A most satisfactory theory of the metastable state formation has been given by Chen (Ref. 10), and the results for $N_2$ are given in Figs. 2(c) and 2(d). There is a second metastable process (Ref. 4) in $N_2$, which has a maximum CS value a full order of magnitude lower than the process at 2.3 eV and is peaked around 5 eV (see the dashed curve peaked at 5 eV in Fig. 4).

In $N_2$, the peak in the elastic CS at low temperature occurring about 1.8 eV is due to 0-0 transitions in the metastable process. For higher temperature, the elastic CS would have to include the effect of the 0-0, 1-1, 2-2, etc., collisions. The 0-0 transition effect is shown in Fig. 3(a) (theoretical)(Ref. 10) and 3(b) (experimental)(Ref. 11), but the 1-1, 2-2, etc., calculated by Chen (Ref. 10) have not been published.

A summary of vibrational cross sections is given in Table 3.

Table 3. Vibrational CS Summary

| Specie | CS | Effect of Gas Temperature | Range of Validity, eV | Remarks |
|---|---|---|---|---|
| $N_2$ | Figs. 2(a), (c), (d) | Pronounced | 0.292 - 4 | Metastable resonance dominated<br>Theory good agreement with experiment |
| $O_2$ | Figs. 2(b) | Harmonic oscillation | 0.196 - 5 | ±30% validity of Fig. 2(b); 1 to 2 orders of magnitude greater than the direct process in $N_2$ |
| NO | -- | -- | -- | Not known |

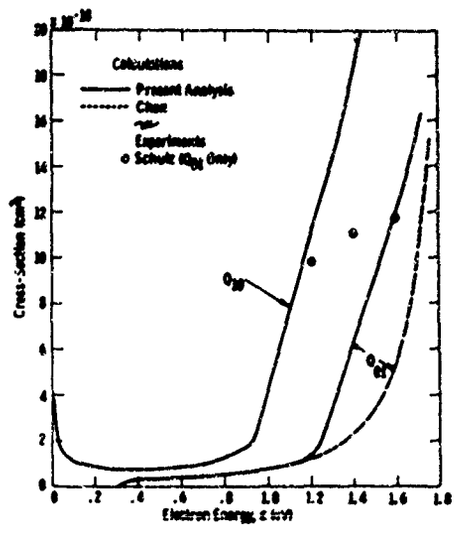


Fig. 2(a). Low-Energy Portion or "Tail" of the v = 1 Vibrational CS($N_2$) in the Region Where the Electron Energy $\epsilon \leq 1.7$ eV (from Ref. 4)

The derived CS $Q_{01}$ for vibrational excitation and the CS $Q_{10}$ for vibrational de-excitation calculated using detailed balancing are shown as solid curves. The curve derived by Chen for $Q_{10}$ is shown as a dashed line. Below 1.2 eV his results and ours are identical. The points represent the experimental results of Schultz for $Q_{01}$ when normalized to our value for the sum of the vibrational excitation CS of 5.5 $\times 10^{-16}$ cm$^2$ at 2.2 eV.

Fig. 2(b). Electron Collision CS in $O_2$ for Momentum Transfer $Q_m$, Vibrational Excitation $Q_{vib}$, Dissociative Attachment $Q_{att}$, Electronic Excitation $Q_{el}$, and Ionization $Q_i$ (from Ref. 9)

Only the sum of the various Electronic CS is shown on this graph.

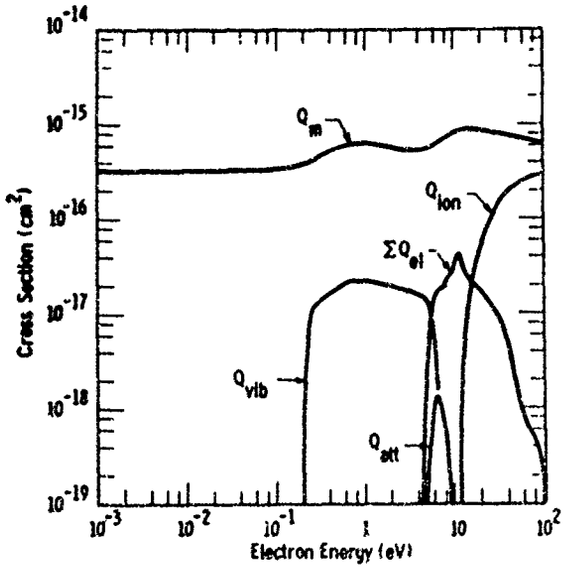

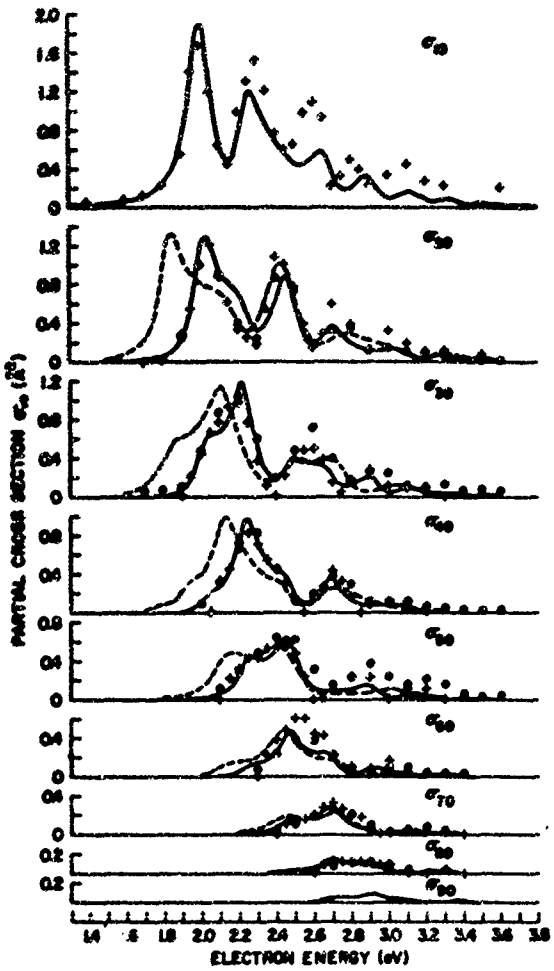


Fig. 2(c). Energy Dependence of the Partial CS for the Excitation of the Ground State $N_2$ Molecule to Various Excited Vibrational States by Slow Electron Impact (from Ref. 10)

The continuous curves are the present calculation, the dashed curves are those calculated by Herzenberg and Mandl, and the circles and the crosses are the experimental data of Schultz measured at the forward angle and at an angle of 72 deg, respectively. Both Schultz's and Herzenberg and Mandl's results are normalized to our calculated absolute orders of magnitude by a common scale factor.

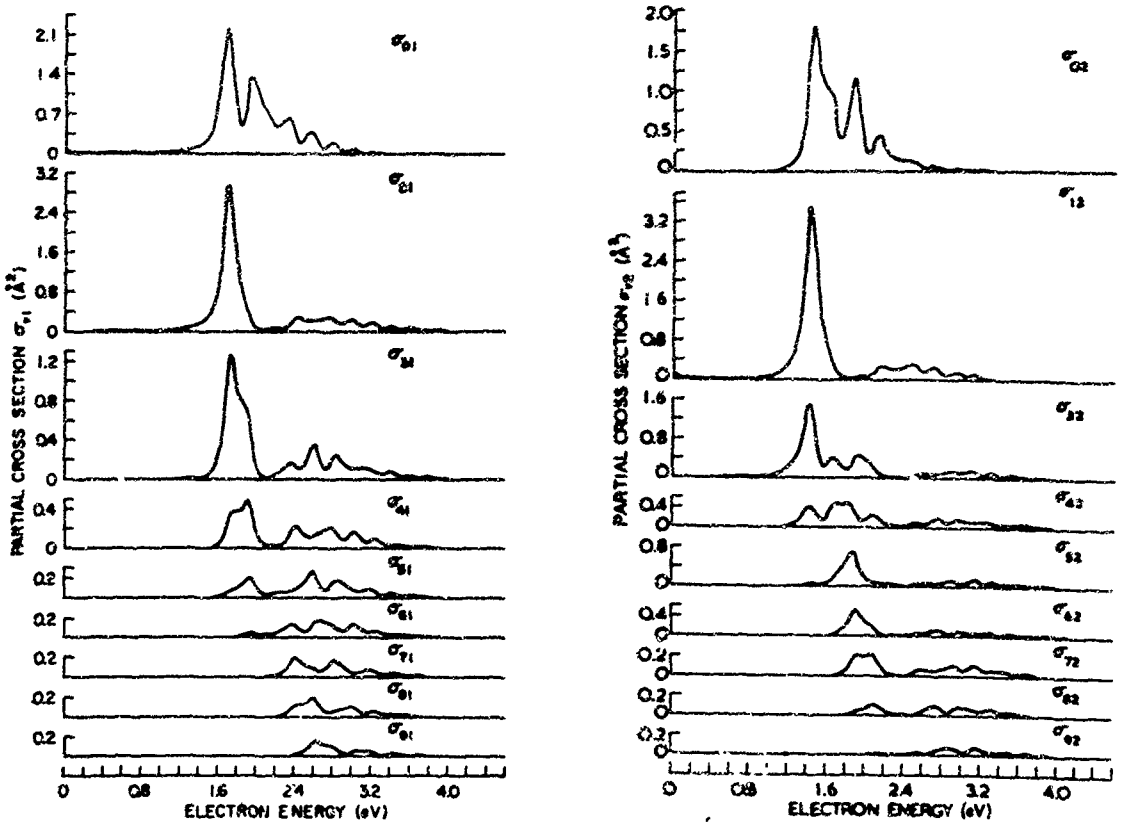


Fig. 2(d). Partial CS for Vibrational Excitation in $N_2$ (from Ref. 10)

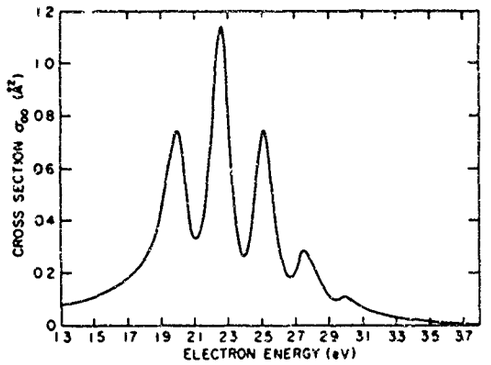


Fig. 3(a). Calculated CS for Elastic Resonance Scattering of Electrons by $N_2$ Molecules as a Function of the Incident Electron Energy (from Ref. 41)

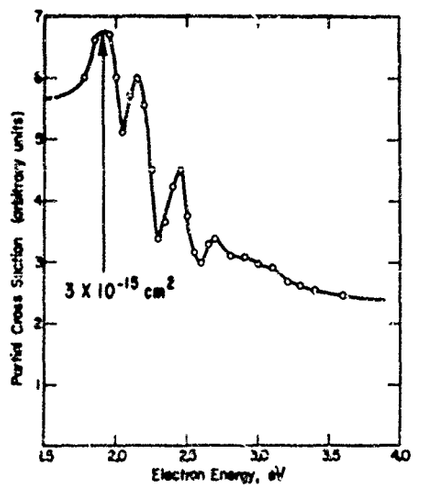


Fig. 3(b). Elastic Scattering of Electrons in $N_2$ at 72° vs Electron Energy in the Energy Range of the Compound State (from Ref. 11)

## V. ELECTRONIC EXCITATION

Electronic excitation in diatomic molecules follows a resonance-type CS with a high energy "tail" (see Ref. 4, Fig. 6 and Fig. 4 of this report). The CS may be approximated by

$$\sigma(E) = \begin{cases} 0 & , \quad E < E_0 \\ \dfrac{\sigma_1}{1 + [(E - E_1)/\Gamma]^2} & , \quad E_0 \le E \le E_2 \\ \dfrac{\sigma_2}{E^n} & , \quad E > E_2 \end{cases} \tag{8}$$

where $E_0$ is the threshold, $\sigma_1$ and $E_1$ are the CS and energy of the maximum, $\Gamma$ is the half-width, $E_2$ is a transition energy, and $\sigma_2$ is adjusted to make a continuous $\sigma(E_2)$. In detail, however, there would be structure in the CS due to the vibrational transitions.

Figure 4 shows various excitation processes found in $N_2$ at low temperatures that Englehart, et al (Ref. 4) used to fit transport data. The solid line CS at 14.5 eV and the CS rising above 20 eV have not been observed but were necessary to obtain agreement in the transport coefficients (Ref. 4). These curves are postulated to be due to dissociation of the molecule, but there is no clear reason for this. There are many possible processes that exist in that energy range; therefore, there is no immediate hope to isolate the processes. However, considering the shape of the CS and their energy positions (Ref. 1), an educated guess would identify this process as $e + N_2 \rightarrow N_2^* + e \rightarrow N + N^* + e$, where $N^*$ is ($^2D$). The order of magnitude of the CS is large but lies between characteristic values for dissociative-recombination and dissociated-attachment.

Little is known about the electronic excitation spectrum in $O_2$ and NO, either experimentally or theoretically. Considering the magnitude of the

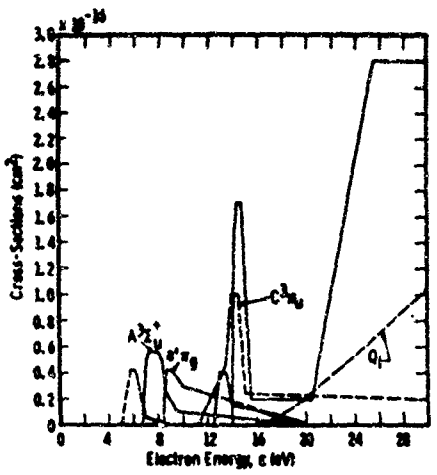


Fig. 4. Effective Excitation CS for $N_2$ with Thresholds Between 5.0 and 14.0 eV and the Ionization CS $Q_i$ (from Ref. 4)

The three excitation processes which have been clearly identified are the $A^3\Sigma_u^+$, the $a^1\pi_g$, and the $C3\pi_u$. These three levels have thresholds at 6.7, 8.4, and 11.2 eV, respectively. The other three, whose exact nature is as yet undetermined, have thresholds at 5.0, 12.5, and 14.0 eV.

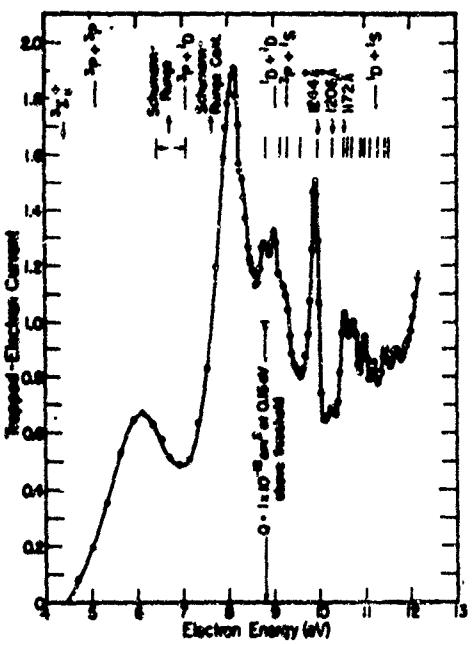


Fig. 5. Excitation Spectrum of $O_2$ Above 4 eV (from Ref. 12)

Peaks observed in optical absorption are indicated. The 1244Å band is called the "longest" band, the 1206Å "second band," and the 1172Å the "third band."

$X^1\Sigma_g^+ \rightarrow C^3\pi_u$ transition in $N_2$ (Ref. 4), one would expect a CS for $X^3\Sigma_g^- \rightarrow a^1\Delta g$ and $b^1\Sigma_g^+$ in $O_2$ somewhat larger than the $10^{-20}$ $cm^2$ order of magnitude values reported by Schulz (Ref. 12). The integrated excitation spectrum for $O_2$ given by the trapped-electron method of Schulz is given in Fig. 5. As an example, Table 4 gives values to use in Eq. (8) to represent the above mentioned $O_2$ transitions.

Table 4. Example Constants for Use in Eqs. (8)

| Transition | $E_o$, eV | $E_1$, eV | $\sigma_1$, $cm^2$ | eV | $E_2$, eV | n |
|---|---|---|---|---|---|---|
| $X^3\Sigma_g^- - a^1\Delta_g$ | 0.98 | 1.14 | $3.1 \times 10^{-20}$ | 0.196 | 1.34 | 1 |
| $X^3\Sigma_g^- - b^1\Sigma_g^+$ | 1.61 | 1.73 | $0.7 \times 10^{-20}$ | 0.196 | 1.92 | 1 |

This table gives a rough functional representation of the CS but does not reflect the structure of the CS. To discuss the temperature dependence of a CS, one must consider the structure; this is done in the discussion surrounding Eq. (9). In Fig. 5, there is a process indicated as peaked at 6 eV with a threshold around 4.5 eV. This process is a form of electronic excitation from $X^3\Sigma_g^-$ to $A^3\Sigma_u^+$ which then dissociates (Ref. 1). From inspection of Fig. 5, the reader may estimate for Eq. (8) $E_o$ = 4.5 eV, $E_1$ = 6 eV, $\Gamma$ = 0.75 eV, $\sigma_1 = 0.68 \times 10^{-18}$ $cm^2$; then $E_2$ and n could be guessed to be 8 eV and 1. Thus, one may see that the assignment of values to the terms of Eq. (8) is a function of the readers ability to sight analyze the CS curve. The representation of Eq. (8) is better for this type of transition, where the upper state is continuous in energy rather than discrete, but it is difficult to take into consideration the effects of temperature without explicit knowledge of the vibrational wave functions involved. The description of how to account for temperature in discrete-discrete transitions follows.

The electronic excitation spectrum of NO in the 5.5 to 9 eV range should be rich due to the presence of a series of optically allowed transitions in this range (Ref. 1); however, no information is available on these transitions. Based on the $a^1\pi_g$ transition in $N_2$, one would imagine that the electronic excitation spectrum of NO would threshold at 5.5 eV, rise to a maximum rapidly, and remain fairly constant around $10^{-16}$ $cm^2$ to about 9 eV, and then drop off above that energy. That is, the CS is comprised of many similar, closely spaced overlapping resonant peaks as given in Eq. (8), instead of representing the envelope of the individual peaks by a function like Eq. (8) as done above for $O_2$.

To discuss the temperature dependence of these electronic excitation processes it is probably best to discuss the behavior of Eq. (8) as the initial state changes due to vibrational excitation and then look at the total CS as a sum of the resultant changed CS.

The principal maximum of the CS, though it should be continuous in energy, will be approximated as a series of closely spaced spikes centered on the upper states vibrational levels.

$$\frac{\sigma_{if}}{\sigma_e} = \sum_{n=0}^{\infty} \left\{ \frac{q_{ni} H\left(E - E_i - E_{T_n}\right)}{1 + \left[(E - E_i - E_n)/\Gamma_n\right]^2} \right\} \tag{9}$$

where $\sigma_e$ is the electronic portion of the CS, $E_i$ is the initial state energy, $E_n$ is the nth excited final state vibrational energy, H(X) is the Heavyside step function, which is zero for X negative and unity for X positive, $E_{T_n}$ is the threshold energy for the nth level, $\Gamma_n$ is given by $(E_{n+1} - E_{n-1})/4$, and $q_{ni}$ is the Franck-Condon factor (vibrational wavefunction overlap integral) for the transition. The $\sigma_{if}$ of Eq. (9) will be the $\sigma_n$ of Eq. (1), and the $\Delta E_n$ will be $E_i - E_{i_o}$, where $i_o$ is the ground state (v = 0) of the ith set of vibrational levels.

For the $N_2$ transition $X^1\Sigma_g^+ \rightarrow A^3\Sigma_u^+$, the threshold is at about 6.2 eV and rises to a peak about 7.5 eV, which corresponds to the maximum of the CS and agrees with the results of Phelps, et al. (Ref. 4) if $\sigma_e$ is chosen as about $5.8 \times 10^{-17}$ $cm^2$. If the above represents the CS from the ground state v = 0, then the v = 1 initial state will lower the threshold by 0.3 eV and the maximum to 6.75 eV and the height of the maximum will be about 6 percent higher. For the v = 2 initial state, the threshold will be at 5.6 eV, the maximum at about 5.85 eV and be about 18 percent larger than the v = 0 CS at its peak. These peak estimates do not include the Boltzmann factor, but do indicate large relative differences at given energies, due principally to a downward shift in energy of the maximum position.

A simpler CS than Eq. (9) could be defined as having the amplitude $\sigma_e q_{ni}$ and be evaluated only at the threshold of the nth level. The resulting CS could then be approximated by straight lines connecting the points. Figure 6 shows this for the $N_2$ transition $X^1\Sigma_g^+ \rightarrow A^3\Sigma_u^-$. For this type of approximation, some high energy tail would have to be added to the bell shaped curve that the aforementioned model would provide. Usually the tails are linearly decreasing or go as $E^{-n/2}$, n integer and fit to the particular transition.

Although it might be useful to include tables of Franck Condon factors in this report, there are so many transitions involved in the molecules $N_2$, $O_2$, and NO that the Franck-Condon factors might fill a large separate document.[1]

---

[1] Franck-Condon Factor Sources: (1) R. W. Nicholls, J. Res. NBS, 65A, (5), 451 (1961): $N_2$ and $N_2^+$. (2) R. W. Nicholls, JQSRT, 4, 433 (1962): $N_2$, $N_2^+$ and $O_2$. (3) P. A. Fraser, et al. Astrophys. J. 122, 55 (1955): $O_2$ and $O_2^+$. (4) P. A. Fraser, et al. Astrophys. J. 119, 286 (1964): $O_2$ and $O_2^+$. (5) R. W. Nicholls, et al. Astrophys. J. 131, 399 (1960): $O_2$ and $O_2^+$. (6) R. W. Nicholls, J. Res. NBS, 68A (5), 535 (1964): NO.

A rather complete bibliography of Franck-Condon factors is presented by R. J. Spindler in JQSRT, 5, 165 (1965).

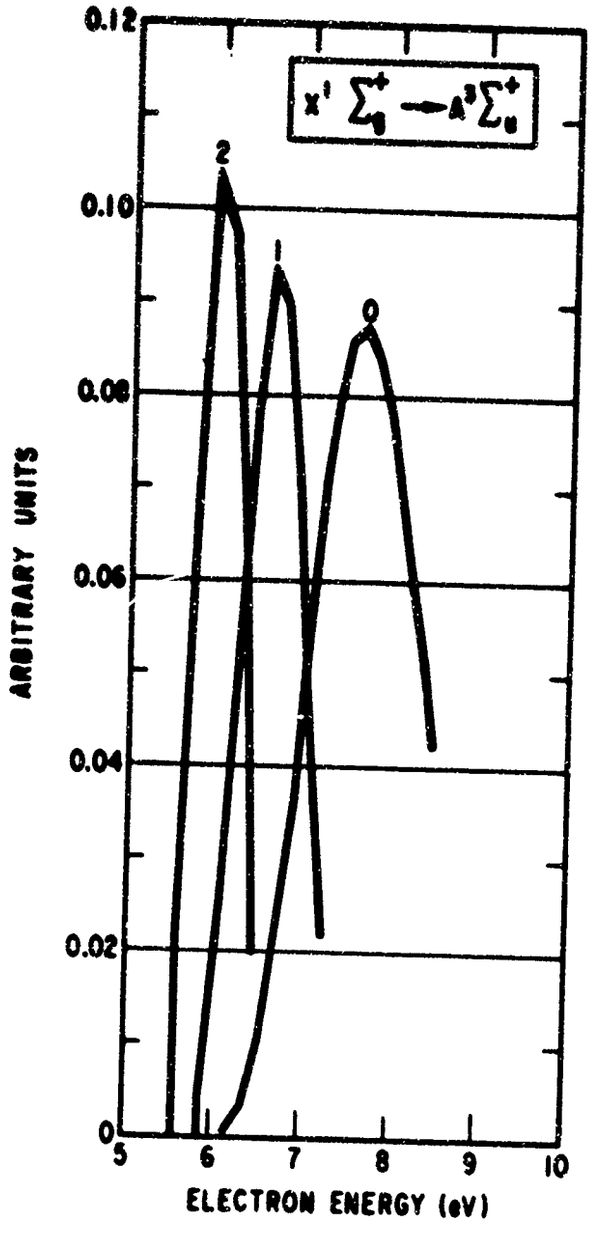


Fig. 6. Partial CS for Excitation in $N_2$

The atoms N and O have the excitation spectrum shown in Figs. 7 and 8 (Ref. 13). For the purpose at hand, transitions from the ground state are all that need be considered because the excited configurations lie too far above the ground state to be significantly populated.

An excitation CS summary is presented in Table 5.

Table 5. Excitation CS Summary

| Specie | CS | Effect of Gas Temperature | Range of Validity, eV | Remarks |
|---|---|---|---|---|
| $N_2$ | Fig. 4 | Franck-Condon Factor Dependent | 5-20 | Rough curves consistent with swarm experiment data |
| $O_2$ | Fig. 5 | Franck-Condon Factor Dependent | 4.5 - 12 | Difficult to separate individual processes from total spectrum |
| NO | -- | -- | -- | Not known |

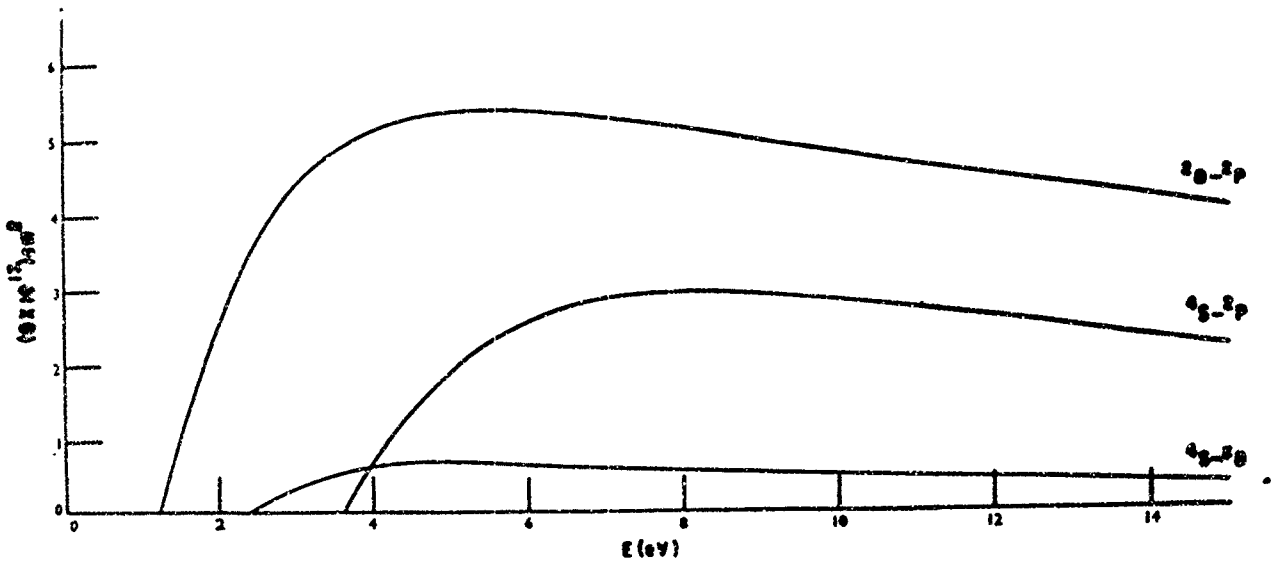


Fig. 7. CS for the Excitation of Metastable Levels of Atomic Nitrogen by Electron Impact From the Results of Seaton (from Ref. 13)

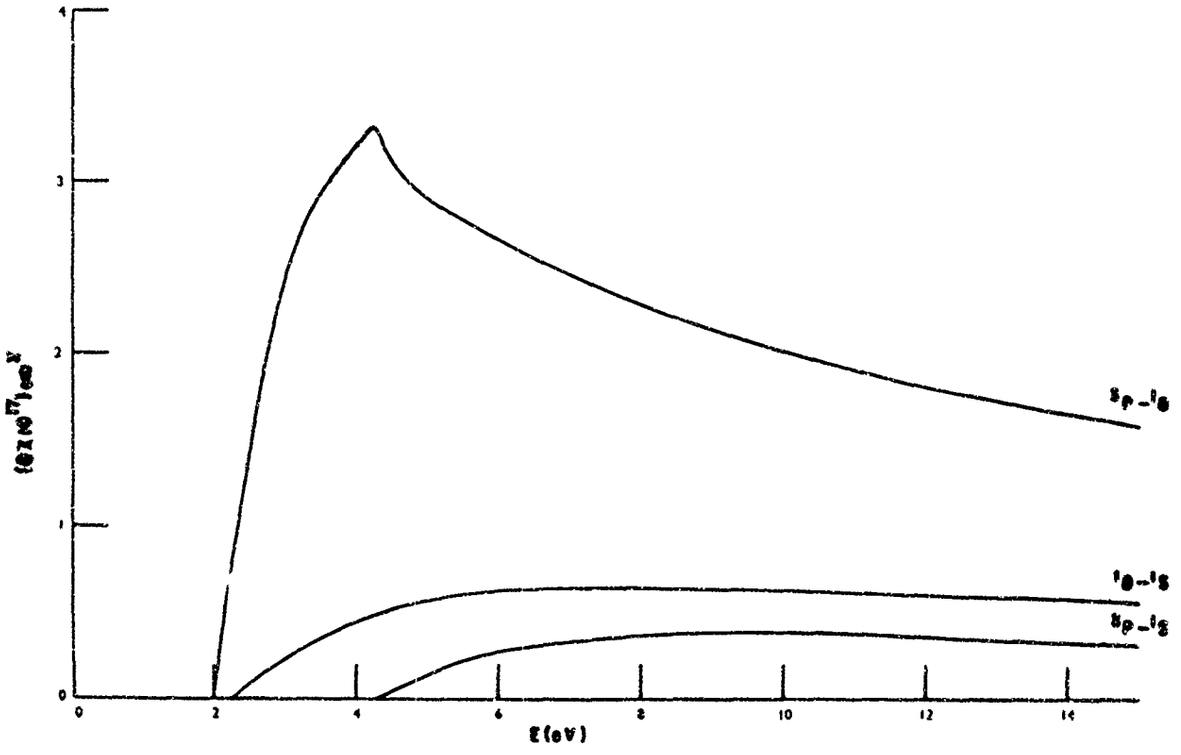


Fig. 8. CS for the Excitation of Metastable Levels of Atomic Oxygen by Electron Impact From the Results of Seaton (from Ref. 13)

## VI. ELECTRON ATTACHMENT

Electron attachment is important principally at very low energies and occurs only in atoms and molecules that form negative ions. For air these are O, $O_2$, and NO. It is difficult to observe radiative attachment ($e + X \rightarrow X^- + h\nu$) because the CS and photon yield is small. The observation technique is to observe the backward process and then calculate the CS for the forward process by the detailed balancing relationship

$$\sigma_c(E) = 9.78 \times 10^{-7}\left(\frac{g_-}{g_o}\right)\sigma_p(E + E_o) \qquad (10)$$

where E is the electron energy, $E_o$ the ion electron binding energy, $g_-$ and $g_o$ the statistical weights (Appendix) of the ionic and neutral species, and $\sigma_p$ is the ion photodetachment CS for photon energy $E + E_o$ (the energies are in eV and the CS in $cm^3$). For $O(^3P)$ and $O^-(^2P)$, $g_o$ and $g_-$ are 9 and 6, respectively (multiplicity times 2L + 1).

Data are available for O (Refs. 14 and 15) and $O_2$ (Ref. 16). The CS presented in Fig. 9 is a direct calculation (Ref. 17), and the CS presented in Fig. 10 is an analytical fit (Ref. 18) to known threshold behavior. There are no data for NO. The expansion of Fig. 10 is valid up to about 4 eV. The CS for $NO^-$ is probably smaller than for $O_2^-$ because the $E_o$ is smaller and behaves in a similar manner. The most that can be said is that $NO^-$ has been seen to exist in mass spectrometer analysis.

Some estimate of the low energy behavior of the attachment CS may be obtained from threshold expansions for photodetachment (Refs. 18 and 19) used with Eq. (10). This shows the attachment CS for O and $O_2$ to behave as $(E + E_o)^3/E$ and $(E + E_o)^3/(E)^{1/2}$, respectively, where E is the electron energy and $E_o$ is the threshold energy. Geltman's theory (Ref. 19) would indicate an $(E + E_o)^3/(E)^{1/2}$ behavior for NO.

Table 6 gives a summary of the electron attachment CS.

Table 6. Radiative Attachment CS Summary

| Specie | CS | Effect of Gas Temperature | Range of Validity, eV | Remarks |
|---|---|---|---|---|
| N | -- | -- | -- | Does not attach |
| $N_2$ | -- | -- | -- | Does not attach |
| O | Fig. 9 | none | 0 - 8 | Radiative attachment from detailed balancing |
| $O_2$ | Fig. 10 | not known | 0 - 4 | |
| NO | -- | -- | -- | Not known |
| A | -- | -- | -- | Does not attach |

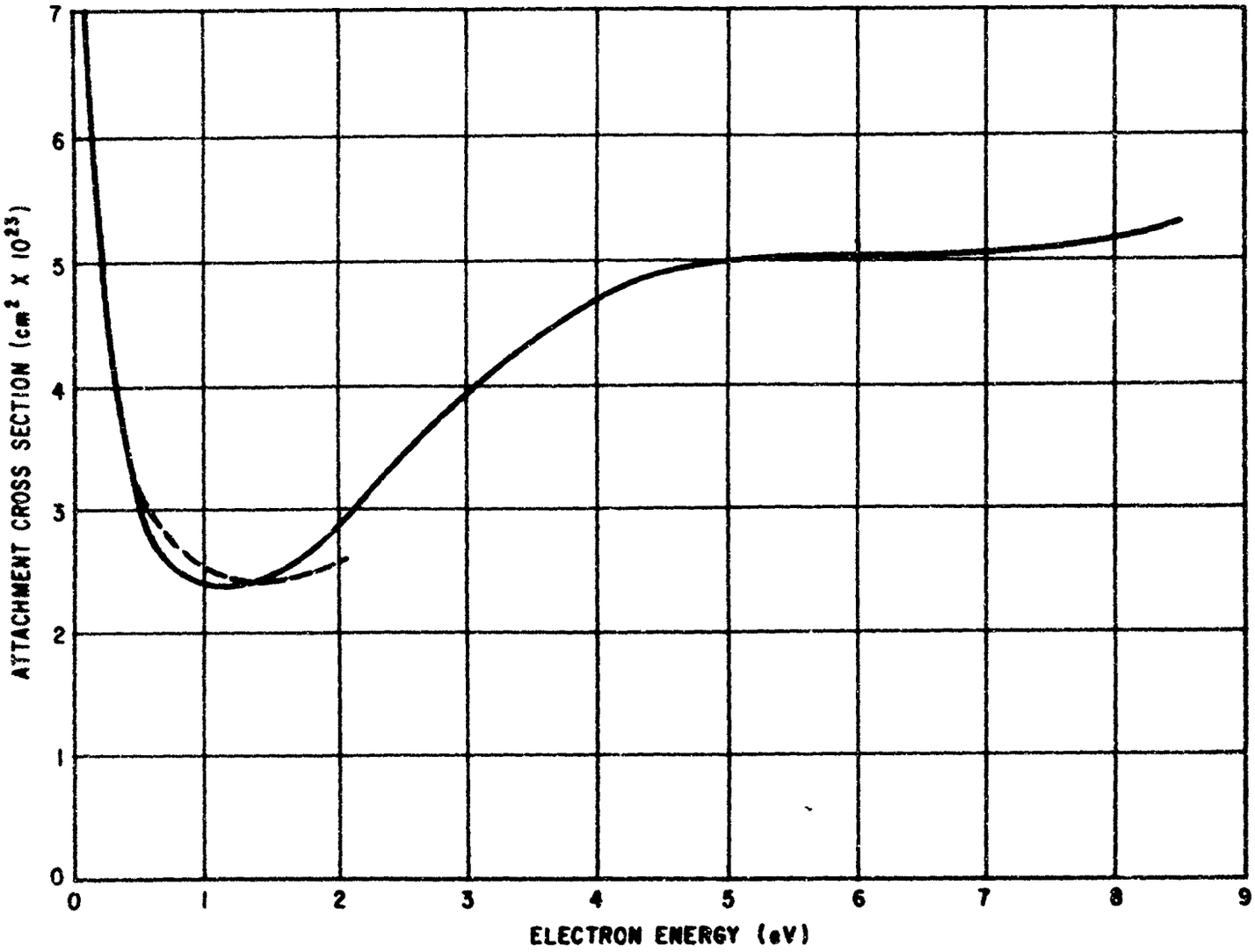


Fig. 9. Attachment CS of Electrons to Atomic Oxygen Calculated by Detailed Balancing from the Photodetachment CS (from Ref. 17)

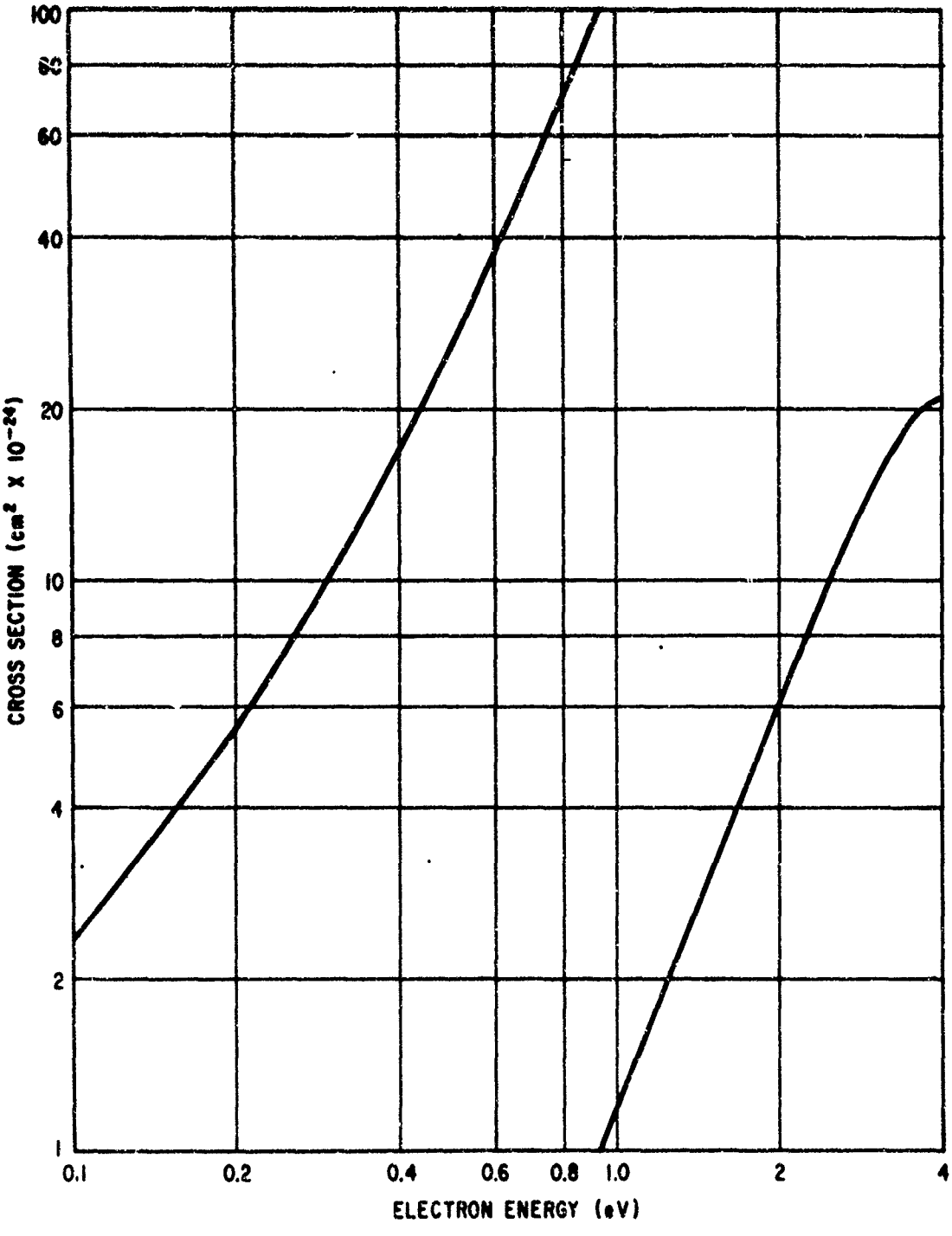


Fig. 10. Radiative Electron Attachment CS in $O_2$

## VII. ELECTRON-MOLECULE DISSOCIATIVE ATTACHMENT

Dissociative attachment CS are not too large, on the order of $10^{-18}$ - $10^{-20}$ $cm^2$. However, the process $e + X_2 \rightarrow X^- + X$ does two things of importance: it eliminates or removes electrons from the gas and it produces energetic by products, the $X^- + X$. For example, the reaction with $O_2$ (Ref. 20) at the peak half heights produces $O + O^-$, sharing about 1.8 to 3.8 eV. Because the process occurs only in species that form negative ions, there is of concern, in addition to $O_2$, only $e + NO \rightarrow N + O^-$. The products of NO, as above, range in the 2.4 to 4.7 eV range. The CS for NO and $O_2$ is given in Figs. 11 to 13.

The CS for the process to lose the electron is shown in Fig. 14 (Ref. 21) and is seen to be substantial; however, the backward process will occur only if the $O^-$ can find another O because of the original energy of separation reducing the likelihood of the original constituents reforming.

The temperature dependence of this type of process (Ref. 22) gives a bell shaped curve like Eq. (8) but with the threshold lowered and the maximum reduced by one over the partition function. The amount of broadening of the threshold is difficult to preduct but will be at least the amount of the vibrational state separation of the lower state.

A dissociative attachment CS summary is presented in Table 7.

Table 7. Dissociative Attachment CS Summary

| Specie | CS | Effect of Gas Temperature | Range of Validity, eV | Remarks |
|---|---|---|---|---|
| NO | Fig. 11 | Squashing of peaks | 1.5 - 14 | Good experimental curve and evidence of rapid detachment by ion-molecule collision |
| $O_2$ | Figs. 12, 13 | Squashing of peaks | 4 - 65 | Same as above |
| $N_2$ | -- | -- | -- | Does not dissociatively attach |

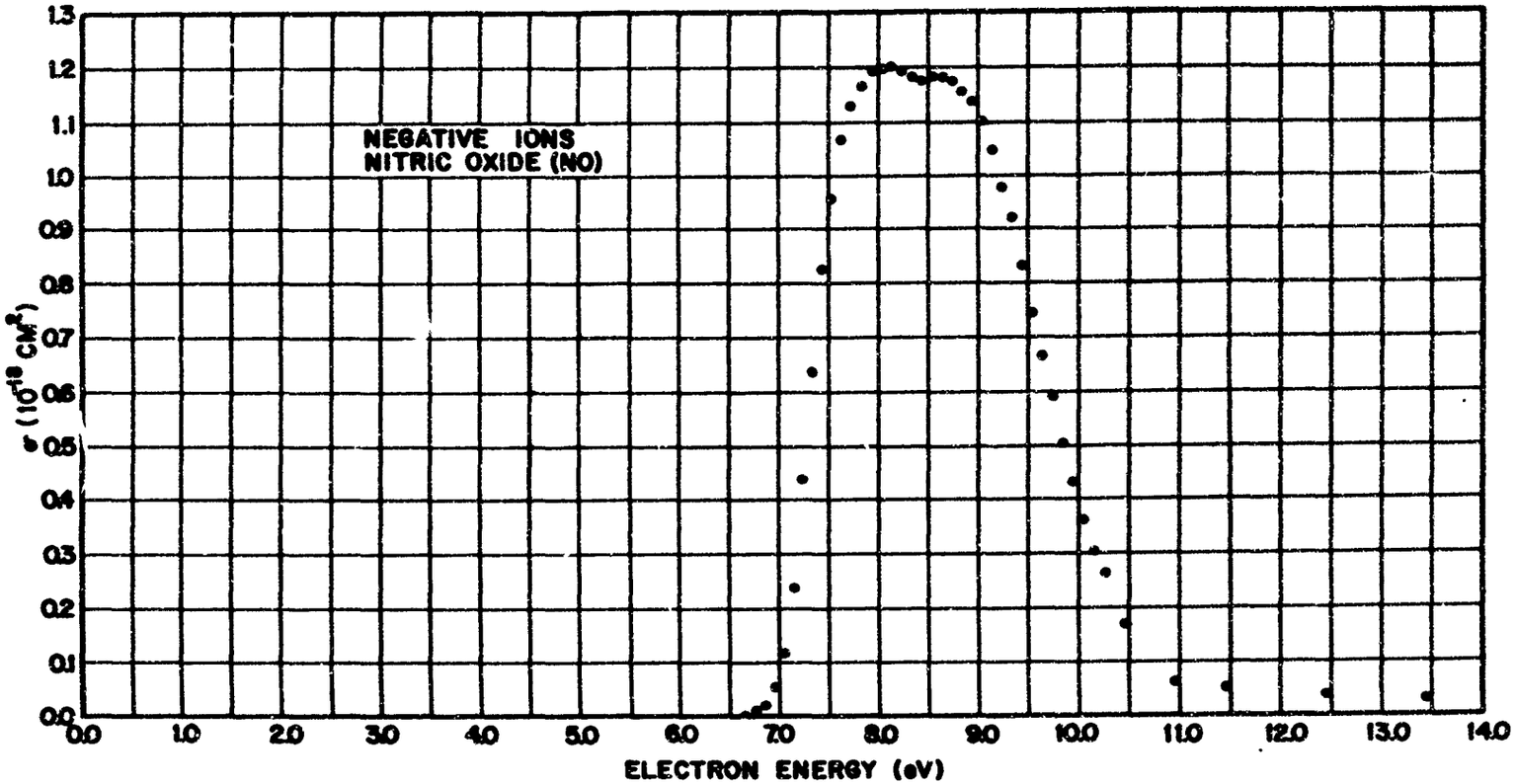


Fig. 11. Dissociative Attachment CS in NO (from Ref. 22)

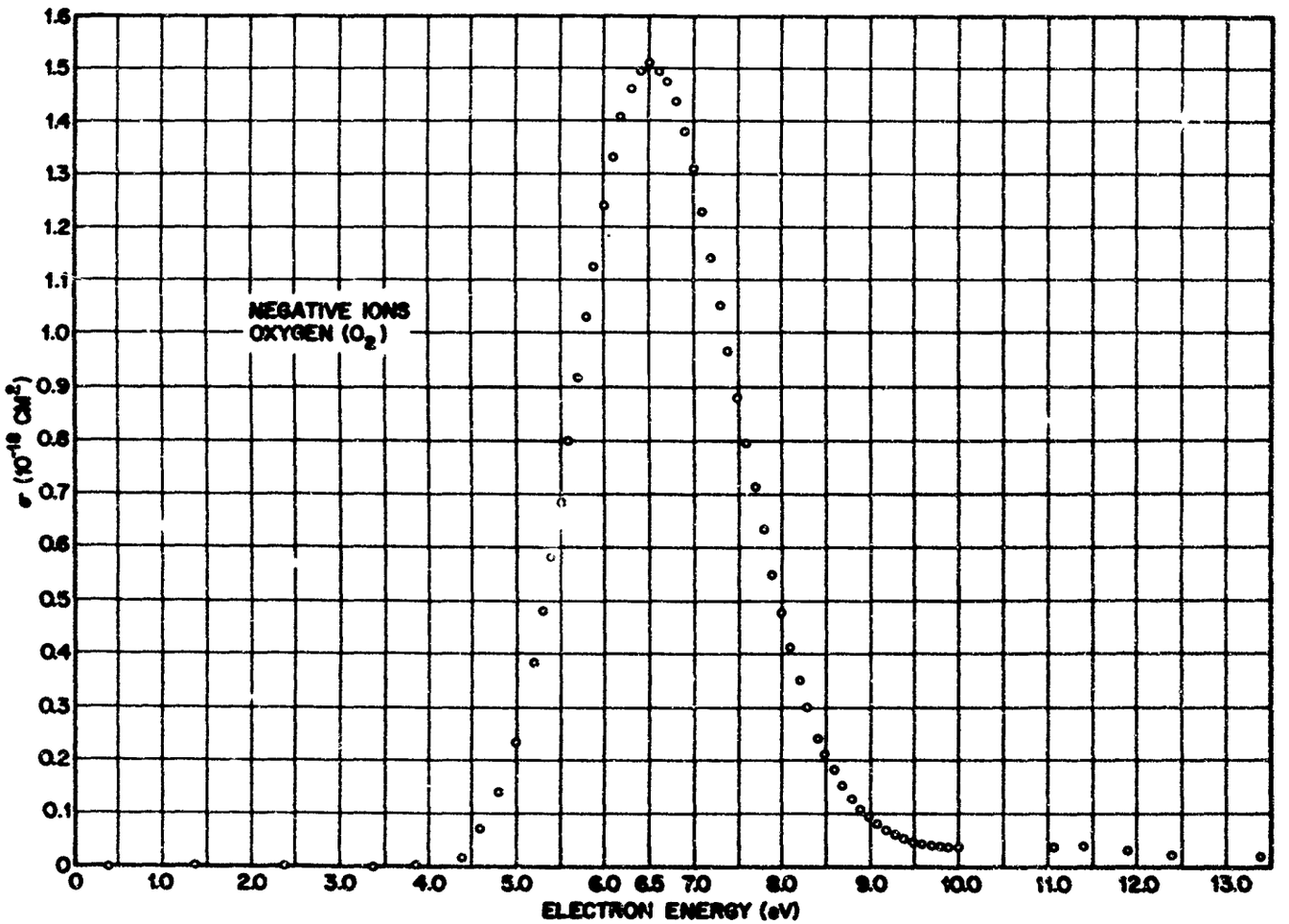


Fig. 12. Dissociative Attachment CS in $O_2$ (from Ref. 22)

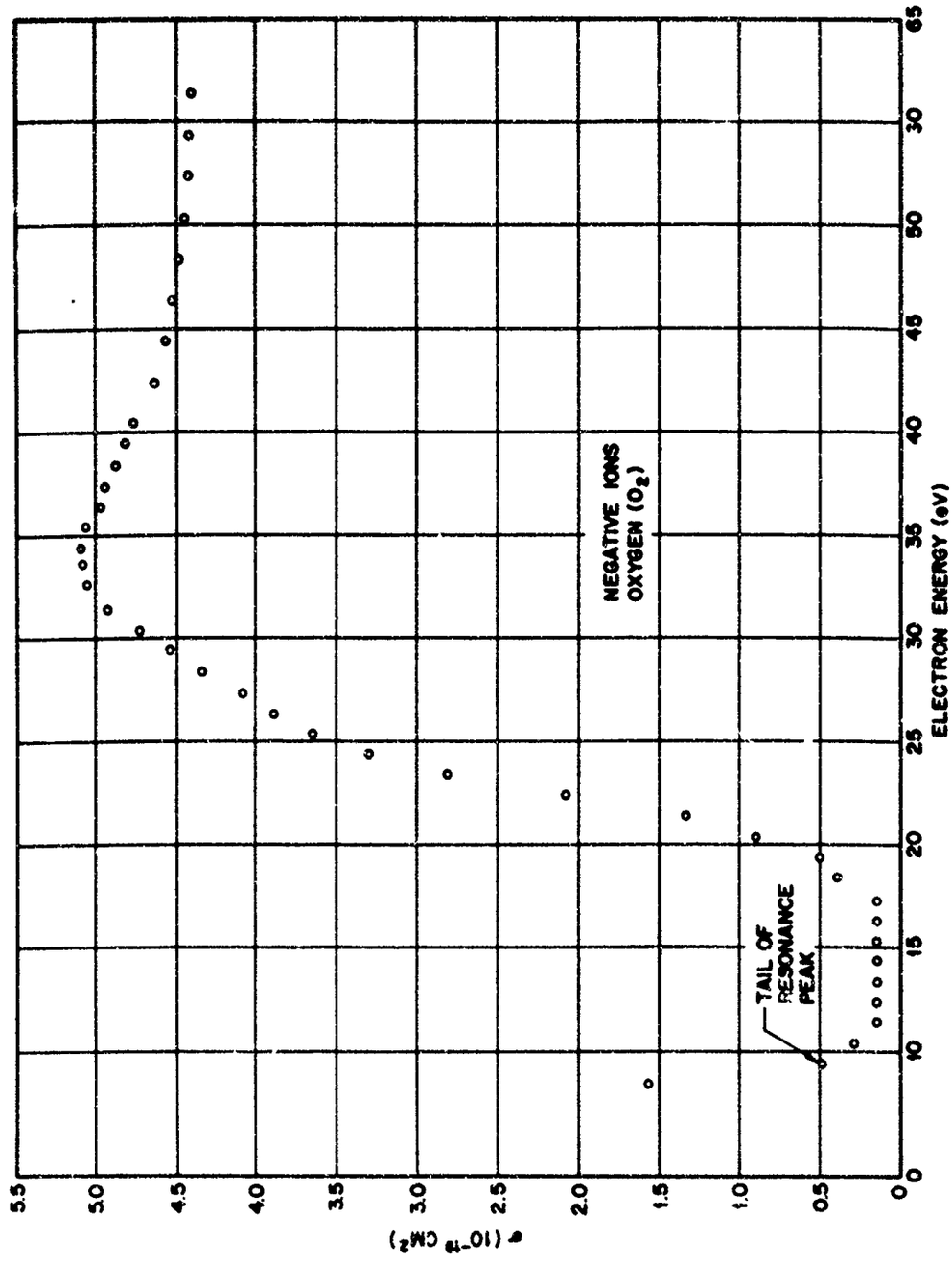


Fig. 13. High Energy Portion of the Dissociative Attachment CS in $O_2$.
(from Ref. 22)

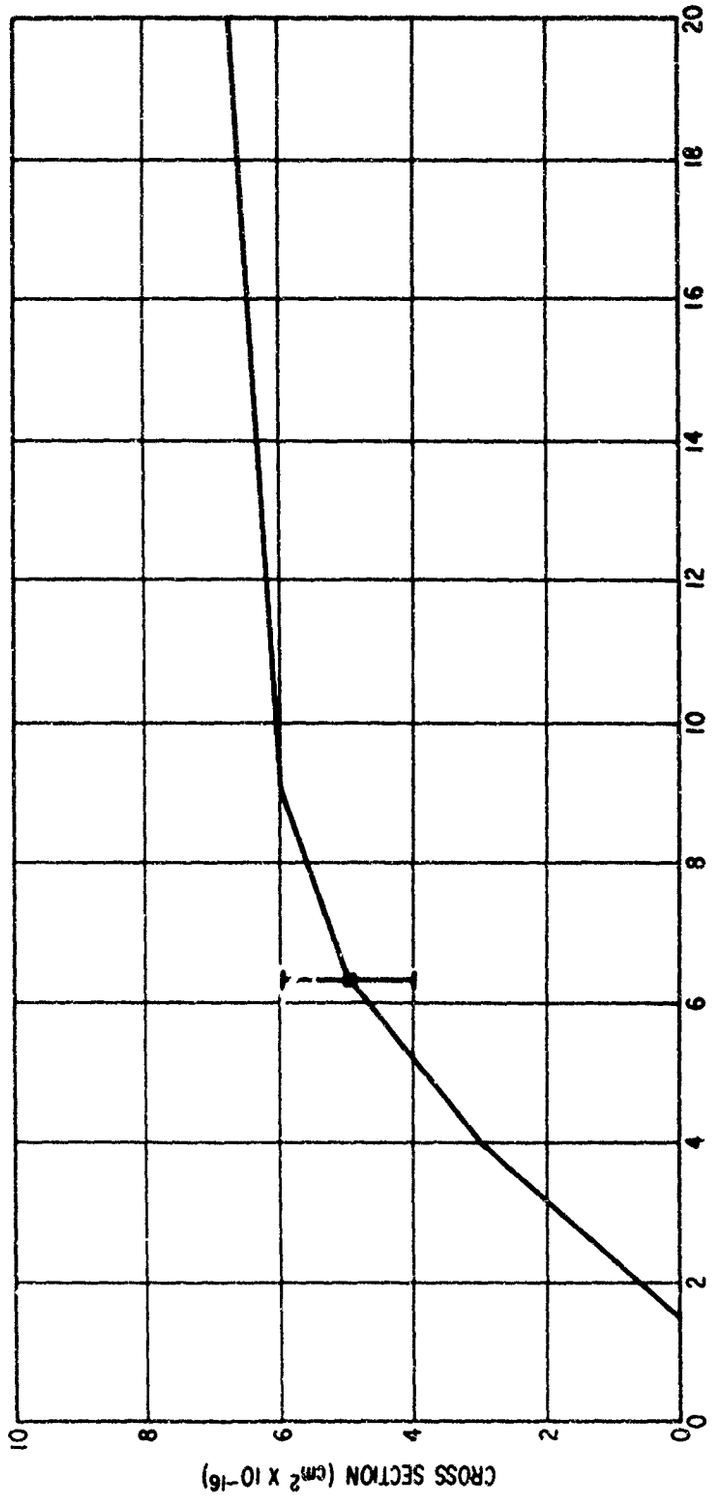


Fig. 14. $O^-$ Deionization CS in $O_2$ (from Ref. 21)

## VIII. IONIZATION BY ELECTRON IMPACT

Electron impact ionization has been thoroughly studied for transitions from the ground state. Results for N, O, A, $N_2$, $O_2$, and NO are given in Figs. 15 through 22 (Refs. 23 through 25).

The general behavior of the CS above threshold is linear in energy and reflects the energy dependence of the electronic contribution. There is presently some dispute as to the threshold behavior (Refs. 26 and 27) of the CS. It is believed that Brion's results are the most refined, which leads to a threshold behavior in the form

$$\sigma_i(E) = \alpha \sum_j (E - E_{T_i} - \Delta E_j) q_{ij} H(E - E_{T_i} - \Delta E_j) \tag{11}$$

where E is the electron energy, $E_{T_i}$ the threshold for ionization from the state i, $\Delta E_j$ the energy of the $j^{\underline{th}}$ state above threshold, $q_{ij}$ the Franck-Condon factor, H(x) is the Heavyside step function, which is zero for x negative and unity for x positive, and $\alpha$ is the slope of the ionization curve taken at large enough E such that $\sum_j q_{ij} \simeq 1$ (that is, in the linear region of the CS). For large enough E, which is usually a few eV above $E_{T_i}$, Eq. (10) becomes

$$\sigma_i(E) \rightarrow \alpha(E - E_{T_i}) - \alpha \sum_j \Delta E_j q_{ij} \tag{12}$$

$$\rightarrow \alpha(E - E_{T_i'})$$

where $E_{T_i'}$ gives an apparent threshold value $E_{T_i} + \Sigma \Delta E_j q_{ij}$.

The temperature dependent ionization CS is then

$$\sigma(E,T) = \frac{1}{P(T)} \sum_i \sigma_i(E) \exp\left(-\frac{\Delta E_i}{kT}\right) \tag{13}$$

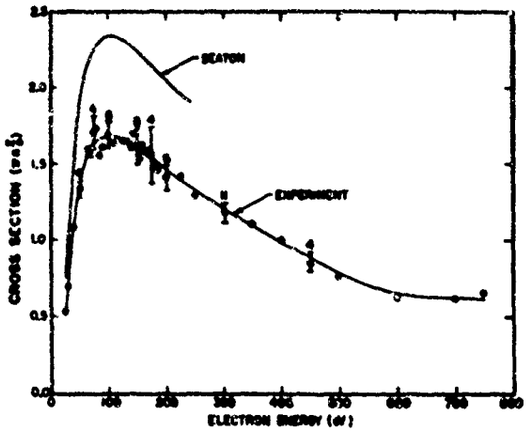


Fig. 15. CS for Ionization of Atomic Nitrogen by Electron Impact (from Ref. 23)

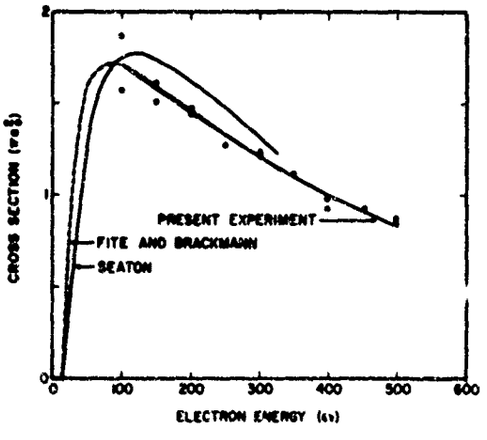


Fig. 16. CS for Ionization of Atomic Oxygen by Electron Impact (from Ref. 24)

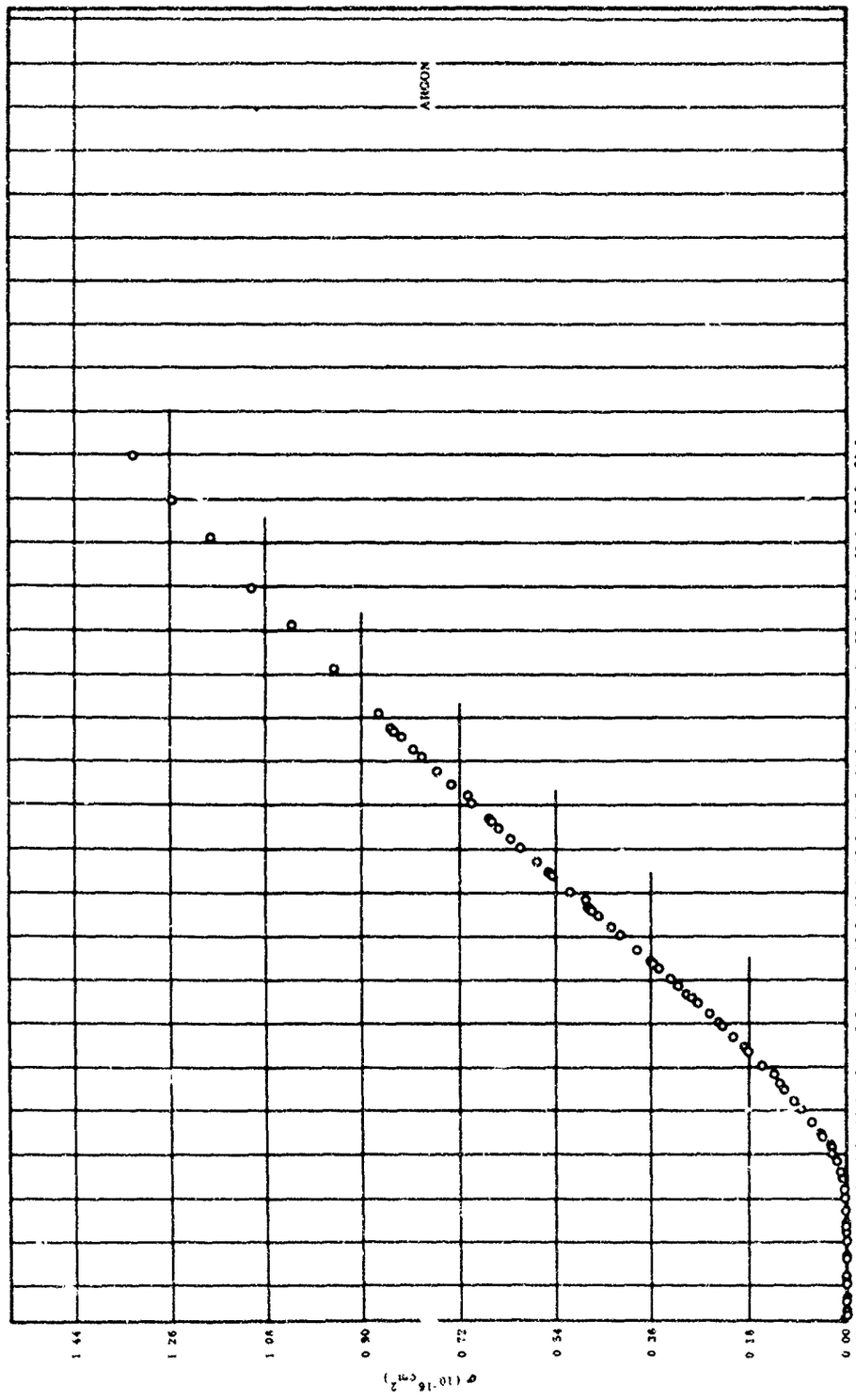


Fig. 17. $\sigma$ vs Electron Energy to 24 eV for Argon (from Ref. 22)
This CS renormalized by a factor of approximately 0.902 (see Ref. 25 for exact values).

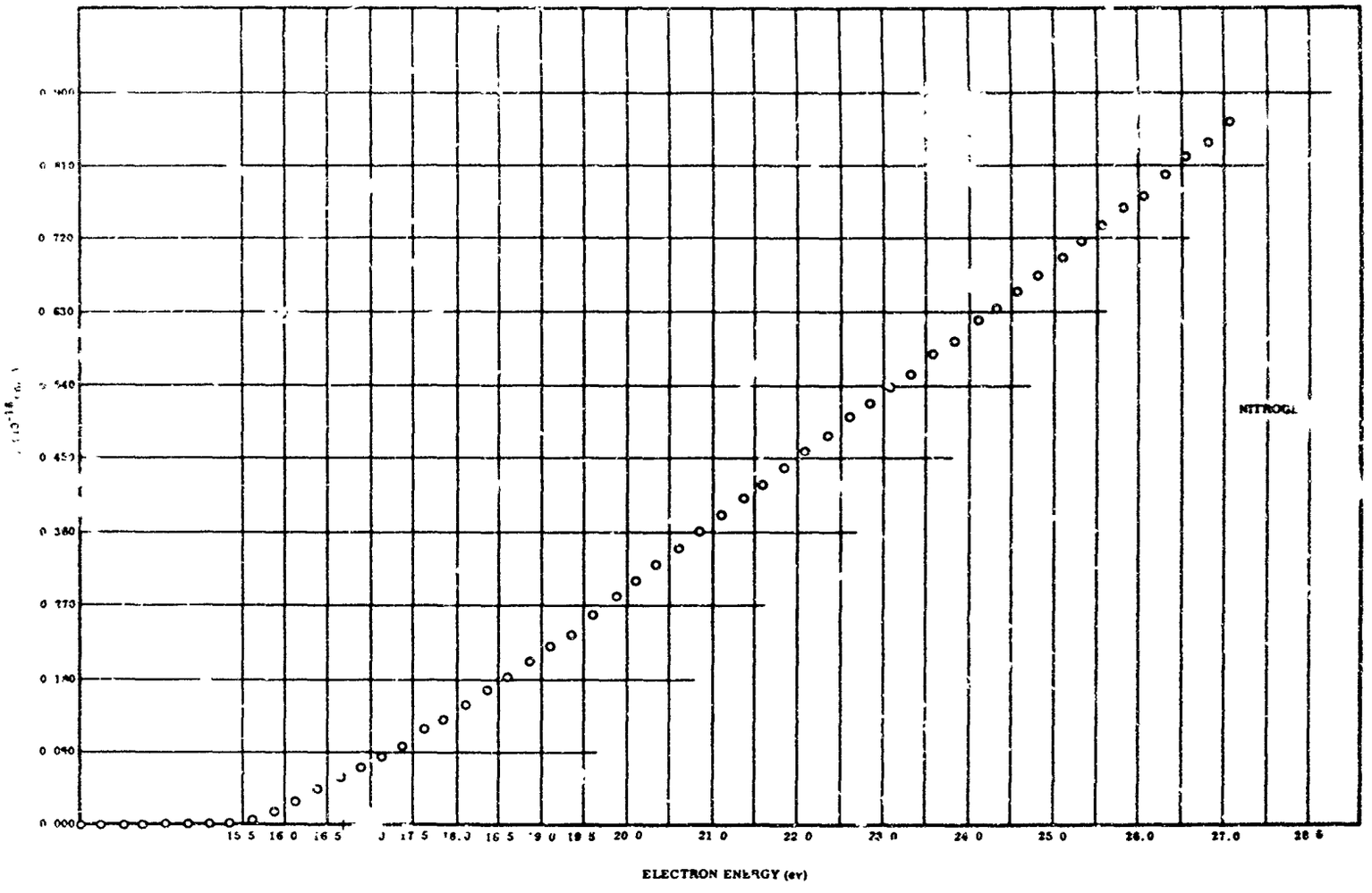


Fig. 18. $\sigma$ vs Electron Energy to Approximately 27 eV for Nitrogen (from Ref. 22)
This CS renorm lized by a factor of approximately 0.925 (see Ref. 25 for exact values).

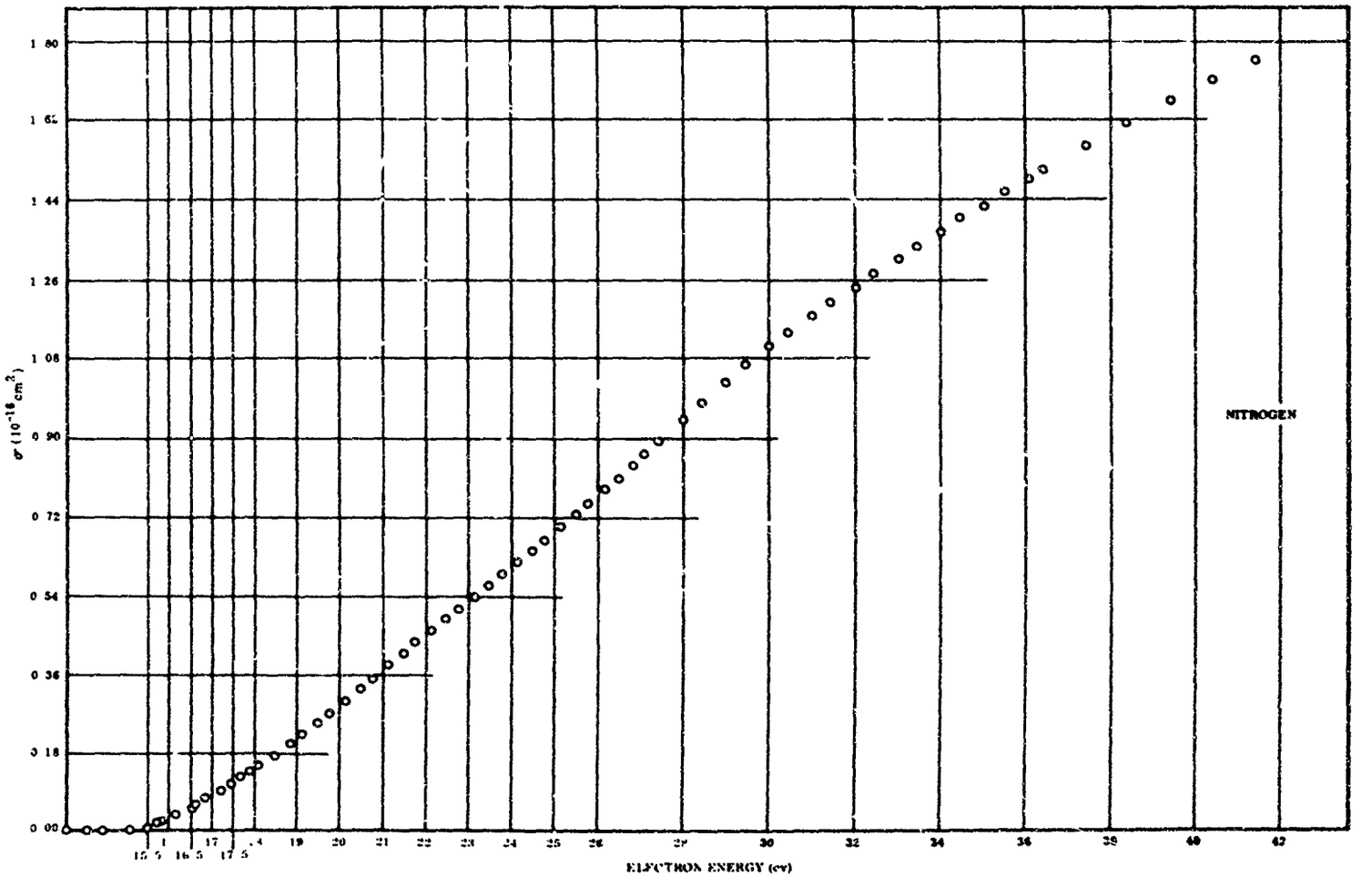


Fig. 19. $\sigma$ vs Electron Energy to Approximately 41.5 eV for Nitrogen (from Ref. 22) This CS renormalized by a factor of approximately 0.925 (see Ref. 25 for exact values).

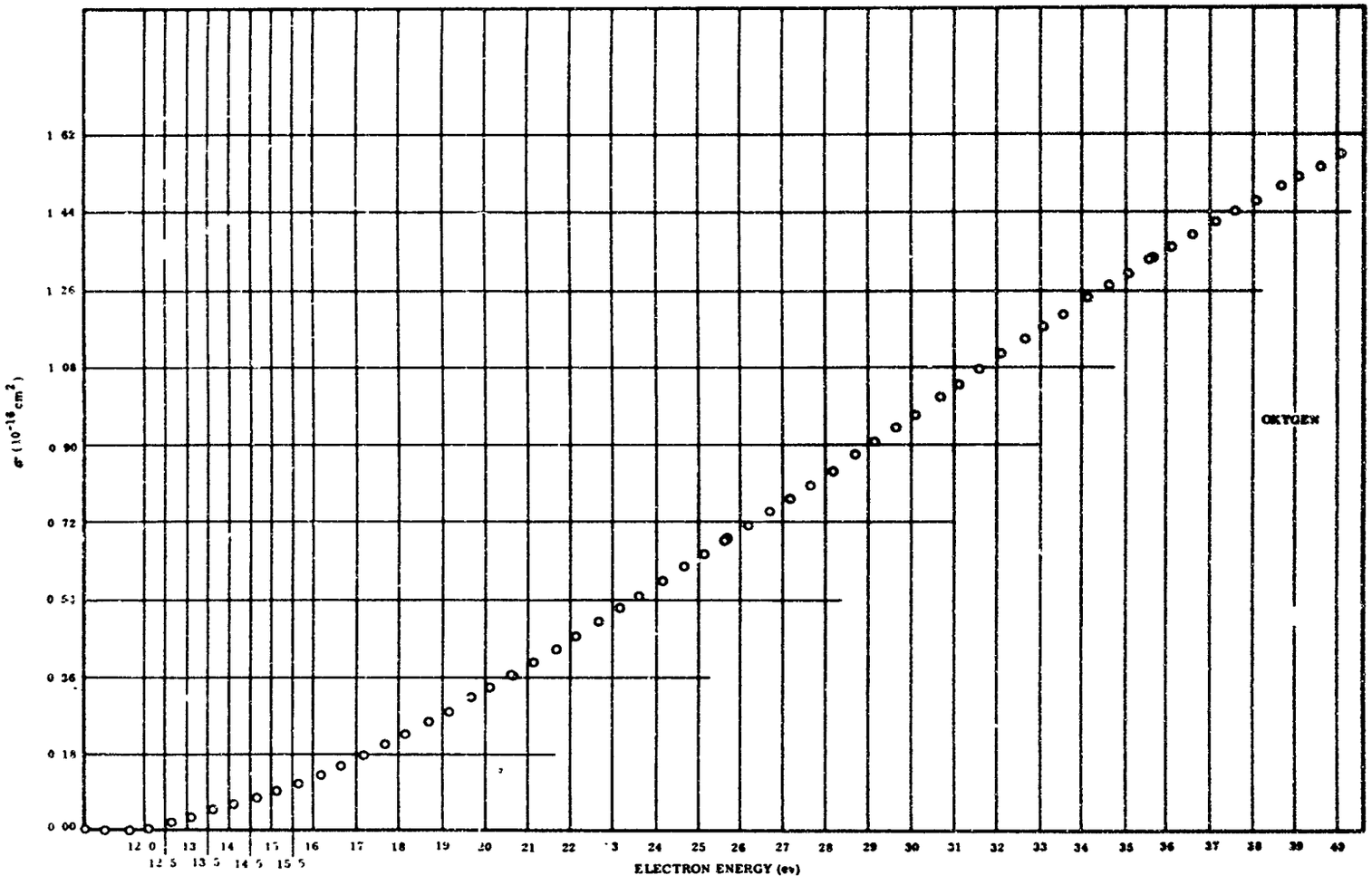


Fig. 20. $\sigma$ vs Electron Energy to Approximately 40 eV for Oxygen (from Ref. 22)

This CS renormalized by a factor of approximately 0.930 (see Ref. 25 for exact values).

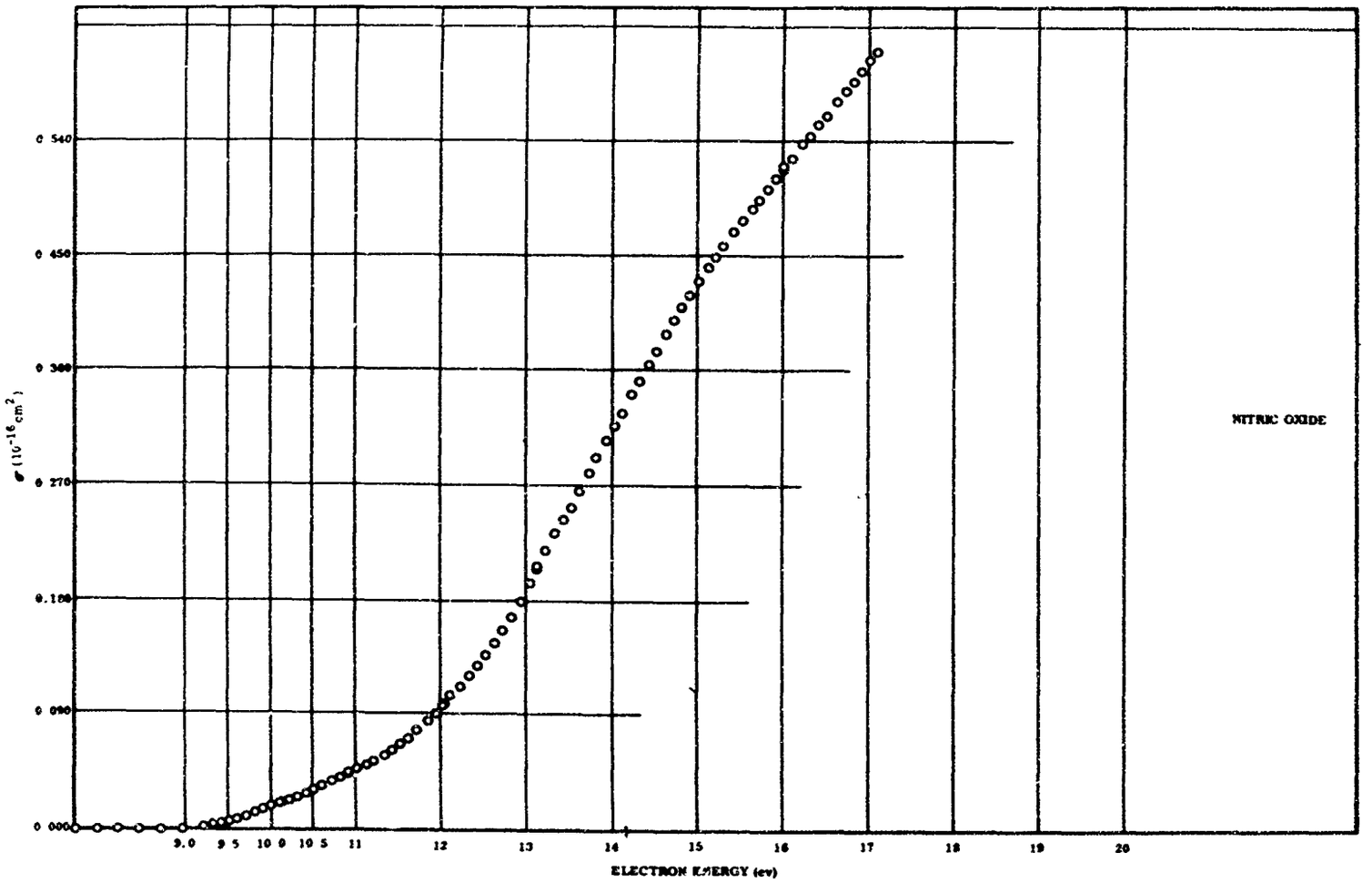


Fig. 21. $\sigma$ vs Electron Energy to Approximately 17 eV for Nitric Oxide (from Ref. 22) This CS renormalized by a factor of approximately 0.930 (see Ref. 25 for exact values).

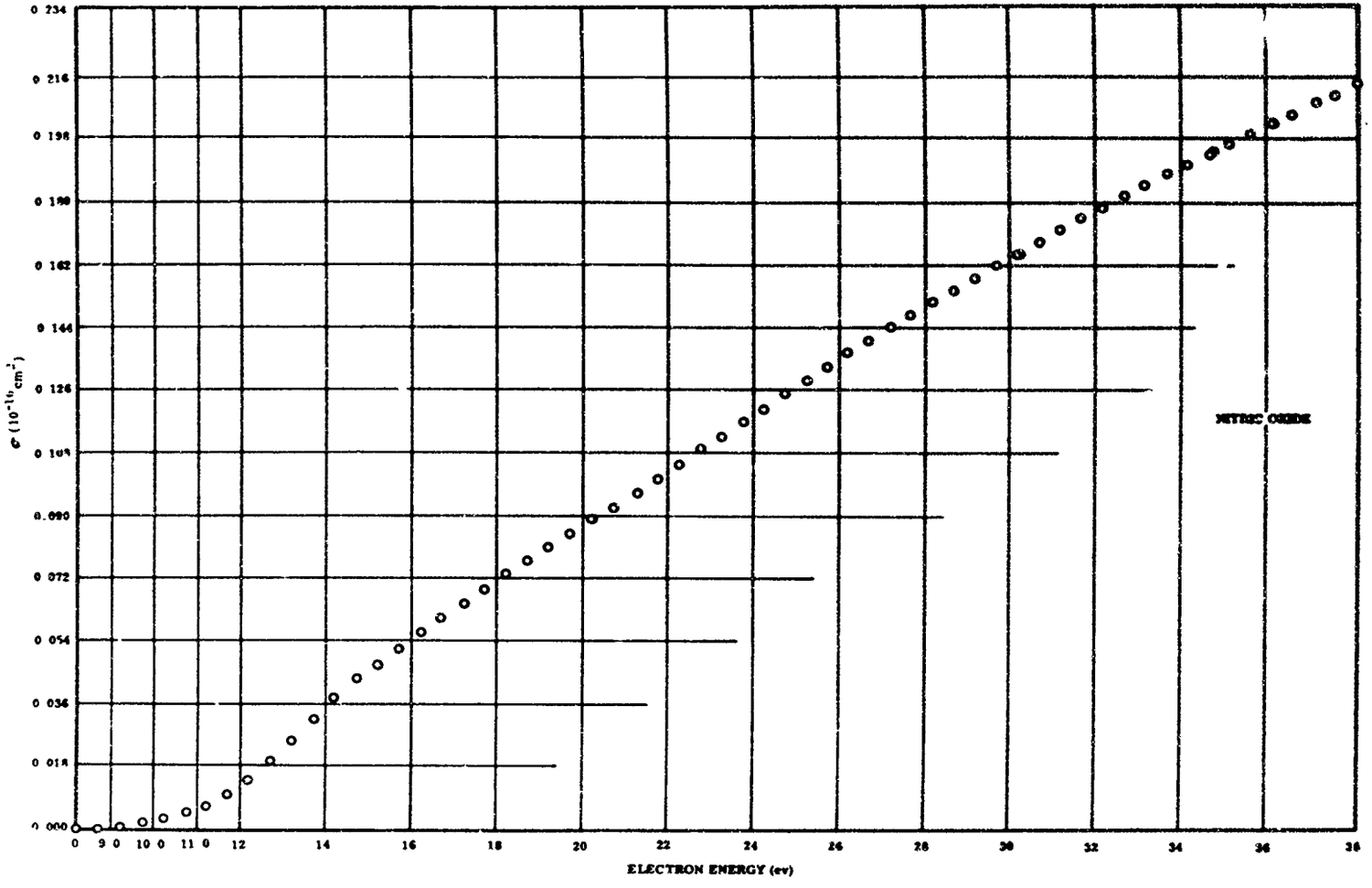


Fig. 22. $\sigma$ vs Electron Energy to 38 eV for Nitric Oxygen (from Ref. 22) This CS renormalized by a factor of approximately 0.930 (see Ref. 25 for exact values).

where $\Delta E_i$ is the excess of energy of the initial state over its ground state.

Tables 8, 9, and 10 give the constants for evaluating Eq. (11) for the threshold ionization of $N_2$, $O_2$ and NO.

Table 8. Ground Electronic State Vibrational Eigenvalues

| v | $E(N_2^+)$, eV | $E(N_2)$, eV | $E(O_2^+)$, eV | $E(O_2)$, eV | $E(NO^+)$, eV | E(NO), eV |
|---|---|---|---|---|---|---|
| 0 | 1.364 - 1 | 1.458 - 1 | 1.158 - 1 | 9.763 - 2 | 1.469 - 1 | 1.176 - 1 |
| 1 | 4.061 - 1 | 4.347 - 1 | 3.445 - 1 | 2.906 - 1 | 4.377 - 1 | 3.503 - 1 |
| 2 | 6.719 - 1 | 7.202 - 1 | 5.690 - 1 | 4.807 - 1 | 7.244 - 1 | 5.795 - 1 |
| 3 | 9.336 - 1 | 1.002 - 0 | 7.894 - 1 | 6.677 - 1 | 1.007 - 0 | 8.053 - 1 |
| 4 | 1.191 - 0 | 1.280 - 0 | 1.006 - 0 | 8.517 - 1 | 1.286 - 0 | 1.028 - 0 |
| 5 | 1.445 - 0 | 1.555 - 0 | 1.218 - 0 | 1.033 - 0 | 1.560 - 0 | 1.246 - 0 |
| 6 | 1.695 - 0 | 1.827 - 0 | 1.426 - 0 | 1.211 - 0 | 1.831 - 0 | 1.462 - 0 |
| 7 | 1.941 - 0 | 2.095 - 0 | 1.630 - 0 | 1.386 - 0 | 2.097 - 0 | 1.674 - 0 |
| 8 | 2.182 - 0 | 2.359 - 0 | 1.830 - 0 | 1.558 - 0 | 2.359 - 0 | 1.882 - 0 |
| 9 | 2.420 - 0 | 2.620 - 0 | 2.026 - 0 | 1.727 - 0 | 2.618 - 0 | 2.087 - 0 |

Note: $1.234 - 5 = 1.234 \times 10^{-5}$

Table 9. Franck-Condon Factors for Ionization

| v | $v'(N_2^+) = 0$ | $v'(O_2^+) = 0$ | $v'(NO^+) = 0$ | $v(N_2^+) = 1$ | $v(O_2^+) = 1$ | $v(NO^+) = 1$ |
|---|---|---|---|---|---|---|
| 0 | 9.017 - 1 | 2.329 - 1 | 1.529 - 1 | 9.472 - 2 | 2.967 - 1 | 2.526 - 1 |
| 1 | 9.125 - 2 | 3.889 - 1 | 3.220 - 1 | 7.183 - 1 | 4.587 - 2 | 1.163 - 1 |
| 2 | 6.616 - 3 | 2.647 - 1 | 2.983 - 1 | 1.658 - 1 | 9.517 - 2 | 9.444 - 3 |
| 3 | 4.673 - 4 | 9.335 - 2 | 1.587 - 1 | 1.905 - 2 | 2.947 - 1 | 1.837 - 1 |
| 4 | 3.753 - 5 | 1.819 - 2 | 5.385 - 2 | 1.842 - 3 | 2.010 - 1 | 2.438 - 1 |
| 5 | 3.574 - 6 | 1.889 - 3 | 1.216 - 2 | 1.810 - 4 | 5.820 - 2 | 1.392 - 1 |
| 6 | 5.310 - 7 | 8.849 - 5 | 1.837 - 3 | 1.957 - 5 | 7.863 - 3 | 4.481 - 2 |
| 7 | 1.323 - 7 | 1.337 - 6 | 1.870 - 4 | 2.376 - 6 | 4.431 - 4 | 8.873 - 3 |
| 8 | 5.428 - 8 | 2.392 - 9 | 1.239 - 5 | 3.221 - 7 | 5.931 - 6 | 1.106 - 3 |
| 9 | 4.224 - 8 | 8.093 - 10 | 4.322 - 7 | 4.794 - 8 | 1.911 - 8 | 8.558 - 5 |

Note: $1.234 - 5 = 1.234 \times 10^{-5}$

| v | $v'(N_2^+) = 2$ | $v'(O_2^+) = 2$ | $v'(NO^+) = 2$ | $v'(N_2^+) = 3$ | $v'(O_2^+) = 3$ | $v'(NO^+) = 3$ |
|---|---|---|---|---|---|---|
| 0 | 3.498 - 3 | 2.237 - 1 | 2.367 - 1 | 6.662 - 5 | 1.306 - 1 | 1.661 - 1 |
| 1 | 1.794 - 1 | 2.683 - 2 | 2.751 - 7 | 1.079 - 2 | 1.233 - 1 | 5.950 - 2 |
| 2 | 5.526 - 1 | 1.6332 - 1 | 1.476 - 1 | 2.519 - 1 | 2.053 - 2 | 8.376 - 2 |
| 3 | 2.230 - 1 | 5.710 - 5 | 5.661 - 2 | 4.069 - 1 | 1.195 - 1 | 2.895 - 2 |
| 4 | 3.635 - 2 | 1.872 - 1 | 3.060 - 2 | 2.627 - 1 | 4.933 - 2 | 1.282 - 1 |
| 5 | 4.539 - 3 | 2.655 - 1 | 2.002 - 1 | 5.729 - 2 | 7.445 - 2 | 4.942 - 3 |
| 6 | 5.434 - 4 | 1.122 - 1 | 2.054 - 1 | 8.897 - 3 | 2.743 - 1 | 9.972 - 2 |
| 7 | 6.883 - 5 | 1.926 - 2 | 9.460 - 2 | 1.264 - 3 | 1.691 - 1 | 2.208 - 1 |
| 8 | 9.549 - 6 | 1.250 - 3 | 2.422 - 2 | 1.841 - 4 | 3.622 - 2 | 1.488 - 1 |
| 9 | 1.454 - 6 | 1.620 - 5 | 3.681 - 3 | 2.875 - 5 | 2.653 - 3 | 4.915 - 2 |

Table 9. Franck-Condon Factors for Ionization (cont.)

| v | $'(N_2^+) = 4$ | $v'(O_2^+) = 4$ | $v'(NO^+) = 4$ | $v'(N_2^+) = 5$ | $v'(O_2^+) = 5$ | $v'(NO^+) = 5$ |
|---|---|---|---|---|---|---|
| 0 | 1.270 - 6 | 6.551 - 2 | 9.759 - 2 | 1.686 - 8 | 2.975 - 2 | 5.086 - 2 |
| 1 | 3.075 - 4 | 1.496 - 1 | 1.255 - 1 | 4.921 - 6 | 1.172 - 1 | 1.328 - 1 |
| 2 | 2.217 - 2 | 1.619 - 2 | 2.632 - 3 | 8.456 - 4 | 8.107 - 2 | 2.527 - 2 |
| 3 | 3.110 - 1 | 8.840 - 2 | 1.092 - 1 | 3.771 - 2 | 5.667 - 3 | 5.819 - 2 |
| 4 | 2.827 - 1 | 3.638 - 2 | 5.012 - 3 | 3.554 - 1 | 1.041 - 1 | 4.653 - 2 |
| 5 | 2.851 - 1 | 1.088 - 1 | 9.823 - 2 | 1.814 - 1 | 5.214 - 4 | 5.546 - 2 |
| 6 | 8.047 - 2 | 1.170 - 1 | 5.896 - 2 | 2.213 - 1 | 1.244 - 1 | 3.163 - 2 |
| 7 | 1.517 - 2 | 2.410 - 1 | 2.190 - 2 | 1.043 - 1 | 1.344 - 3 | 1.055 - 1 |
| 8 | 2.513 - 3 | 2.197 - 1 | 1.858 - 1 | 2.347 - 2 | 1.866 - 1 | 3.300 - 4 |
| 9 | 4.149 - 4 | 5.793 - 2 | 1.922 - 1 | 4.476 - 3 | 2.588 - 1 | 1.227 - 1 |
| 10 | -- | 4.700 - 3 | 8.234 - 2 | 8.292 - 4 | 8.309 - 2 | 2.137 - 1 |
| 11 | -- | 4.828 - 5 | 1.826 - 2 | -- | 7.332 - 3 | 1.201 - 1 |
| 12 | -- | -- | 2.214 - 3 | -- | 5.916 - 5 | 3.207 - 2 |
| 13 | -- | -- | 1.430 - 4 | -- | -- | 4.472 - 3 |
| 14 | -- | -- | -- | -- | -- | 3.201 - 4 |

Table 10. Factors in Eq. (11)

| $v_i$ | $q_{oi}(N_2)$ | $E_i q_{oi}(N_2)$ | $q_{oi}(O_2)$ | $E_i q_{oi}(O_2)$ | $q_{oi}(NO)$ | $E_i q_{oi}(NO)$ |
|---|---|---|---|---|---|---|
| 0 | 9.017 - 1 | 1.230 - 1 | 2.329 - 1 | 2.700 - 2 | 1.529 - 1 | 2.247 - 2 |
| 1 | 9.929 - 1 | 1.600 - 1 | 6.218 - 1 | 1.609 - 1 | 4.750 - 1 | 1.634 - 1 |
| 2 | 1.000 | 1.645 - 1 | 8.865 - 1 | 3.115 - 1 | 7.732 - 1 | 3.795 - 1 |
| 3 | 1.000 | 1.649 - 1 | 9.798 - 1 | 3.852 - 1 | 9.320 - 1 | 5.393 - 1 |
| 4 | -- | -- | 9.980 - 1 | 4.035 - 1 | 9.858 - 1 | 6.086 - 1 |
| 5 | -- | -- | 9.999 - 1 | 4.058 - 1 | 9.980 - 1 | 6.275 - 1 |
| 6 | -- | -- | 1.000 | 4.060 - 1 | 9.998 - 1 | 6.309 - 1 |
| 7 | -- | -- | -- | -- | 1.000 | 6.313 - 1 |

Note: $1.234 - 5 = 1.234 \times 10^{-5}$

| $v_i$ | $q_{1i}(N_2)$ | $E_i q_{1i}(N_2)$ | $q_{1i}(O_2)$ | $E_i q_{1i}(O_2)$ | $q_{1i}(NO)$ | $E_i q_{1i}(NO)$ |
|---|---|---|---|---|---|---|
| 0 | 9.472 - 2 | 1.292 - 2 | 2.967 - 1 | 3.437 - 2 | 2.526 - 1 | 3.711 - 2 |
| 1 | 8.130 - 1 | 3.046 - 1 | 3.425 - 1 | 5.017 - 2 | 3.689 - 1 | 8.802 - 2 |
| 2 | 9.788 - 1 | 4.160 - 1 | 4.377 - 1 | 1.043 - 1 | 3.783 - 1 | 9.486 - 2 |
| 3 | 9.979 - 1 | 4.338 - 1 | 7.324 - 1 | 3.370 - 1 | 5.621 - 1 | 2.799 - 1 |
| 4 | 9.997 - 1 | 4.360 - 1 | 9.335 - 1 | 5.392 - 1 | 8.059 - 1 | 5.933 - 1 |
| 5 | 9.999 - 1 | 4.363 - 1 | 9.917 - 1 | 6.101 - 1 | 9.451 - 1 | 8.105 - 1 |
| 6 | 9.999 - 1 | 4.363 - 1 | 9.995 - 1 | 6.213 - 1 | 9.899 - 1 | 8.926 - 1 |
| 7 | -- | -- | 1.000 | 6.220 - 1 | 9.988 - 1 | 9.112 - 1 |
| 8 | -- | -- | -- | -- | 9.999 - 1 | 9.138 - 1 |
| 9 | -- | -- | -- | -- | 1.000 | 9.140 - 1 |

Table 10. Factors in Eq. (11) (cont.)

| $v_i$ | $q_{2i}(N_2)$ | $E_i q_{2i}(N_2)$ | $q_{2i}(O_2)$ | $E_i q_{2i}(O_2)$ | $q_{2i}(NO)$ | $E_i q_{2i}(NO)$ |
|---|---|---|---|---|---|---|
| 0 | 3.498 - 3 | 4.771 - 4 | 2.237 - 1 | 2.592 - 2 | 2.367 - 1 | 3.477 - 2 |
| 1 | 1.828 - 1 | 7.332 - 2 | 2.506 - 1 | 3.516 - 2 | 2.367 - 1 | 3.477 - 2 |
| 2 | 7.355 - 1 | 4.446 - 1 | 4.139 - 1 | 1.281 - 1 | 3.843 - 1 | 1.417 - 1 |
| 3 | 9.585 - 1 | 6.528 - 1 | 4.139 - 1 | 1.281 - 1 | 4.409 - 1 | 1.987 - 1 |
| 4 | 9.949 - 1 | 6.961 - 1 | 6.018 - 1 | 3.170 - 1 | 4.715 - 1 | 1.987 - 1 |
| 5 | 9.994 - 1 | 7.027 - 1 | 8.673 - 1 | 6.404 - 1 | 6.718 - 1 | 2.381 - 1 |
| 6 | 9.999 - 1 | 7.036 - 1 | 9.795 - 1 | 8.004 - 1 | 8.771 - 1 | 5.505 - 1 |
| 7 | 1.000 | 7.038 - 1 | 9.987 - 1 | 8.318 - 1 | 9.718 - 1 | 9.265 - 1 |
| 8 | -- | -- | 1.000 | 8.341 | 9.960 - 1 | 1.125 |
| 9 | -- | -- | 1.000 | 8.342 | 9.997 - 1 | 1.182 |
| 10 | -- | -- | -- | -- | 1.000 | 1.192 |

| $v_i$ | $q_{3i}(N_2)$ | $E_i q_{3i}(N_2)$ | $q_{3i}(O_2)$ | $E_i q_{3i}(O_2)$ | $q_{3i}(NO)$ | $E_i q_{3i}(NO)$ |
|---|---|---|---|---|---|---|
| 0 | 6.662 - 5 | 9.085 - 6 | 1.306 - 1 | 1.513 - 2 | 1.661 - 1 | 2.440 - 2 |
| 1 | 1.086 - 2 | 4.393 - 3 | 2.539 - 1 | 5.761 - 2 | 2.256 - 1 | 5.045 - 2 |
| 2 | 2.628 - 1 | 1.737 - 1 | 2.745 - 1 | 6.929 - 2 | 3.094 - 1 | 1.111 - 1 |
| 3 | 6.696 - 1 | 5.535 - 1 | 3.939 - 1 | 1.6[illegible] - 1 | 3.383 - 1 | 1.403 - 1 |
| 4 | 9.323 - 1 | 8.665 - 1 | 4.433 - 1 | 2.132 - 1 | 4.666 - 1 | 3.051 - 1 |
| 5 | 9.896 - 1 | 9.493 - 1 | 5.177 - 1 | 3.039 - 1 | 4.715 - 1 | 3.128 - 1 |
| 6 | 9.985 - 1 | 9.643 - 1 | 7.920 - 1 | 6.950 - 1 | 5.712 - 1 | 4.954 - 1 |
| 7 | 9.998 - 1 | 9.668 - 1 | 9.611 - 1 | 9.707 - 1 | 7.920 - 1 | 9.584 - 1 |
| 8 | 1.000 | 9.672 - 1 | 9.973 - 1 | 1.037 | 9.408 - 1 | 1.309 |
| 9 | -- | -- | 1.000 | 1.042 | 9.899 - 1 | 1.438 |
| 10 | -- | -- | -- | -- | 9.990 - 1 | 1.464 |
| 11 | -- | -- | -- | -- | 9.999 - 1 | 1.467 |
| 12 | -- | -- | -- | -- | 1.000 | 1.467 |

Examples of the partial CS for NO in the ground electronic state as given by Eq. (11) are presented in Fig. 23. Tables 8 through 10 give values of $E_i$, the lower state eigenvalues, $E_j$ the upper state eigenvalues; $q_{ij}$ the Franck-Condon factors, the sums $\sum_i q_{ij}$ and $\sum_j \Delta E_j q_{ij}$, the thresholds and the slopes $\alpha$ so that detailed CS may be calculated for desired processes according to Eq. (10).

Electron dissociative ionization ($e + X_2 \rightarrow X + X^+ + 2e$) is also an ionization process. The CS for $N_2$, NO, and $O_2$ are shown in Figs. 24 through 26. The curves are presented for ions and atoms coming apart with energy greater than 0.25 eV. Considering the kinetic energy of separation in these processes (Ref. 1), this represents nearly all the ions and reflects an accurate CS.

An electron impact ionization CS summary is presented in Table 11.

Table 11. Electron Impact Ionization CS Summary

| Specie | CS | Effect of Gas Temperature | Range of Validity, eV | Remarks |
|---|---|---|---|---|
| N | Fig. 15 | None for temperatures <10,000°K | 14.5 | Linear (E) threshold behavior |
| O | Fig. 16 | | 13.55 | Linear (E) threshold behavior |
| A | Fig. 17 | | 15.75 - 24 | Linear (E) threshold behavior |
| $N_2$ | Figs. 18, 19 | Franck-Condon | 15.6 - 42 | Threshold dependence on gas temperature somewhat less than NO |
| $O_2$ | Fig. 20 | Factor | 12.1 - 40 | Same as above |
| NO | Figs. 21, 22 | Dependent | 9.25 - 38 | Pronounced threshold dependence on gas temperature |
| $N_2$ | Fig. 24 | Not known | 25 - 48 | |
| $O_2$ | Fig. 25 | Not known | 20 - 48 | |
| NO | Fig. 26 | Not known | 22 - 44 | |

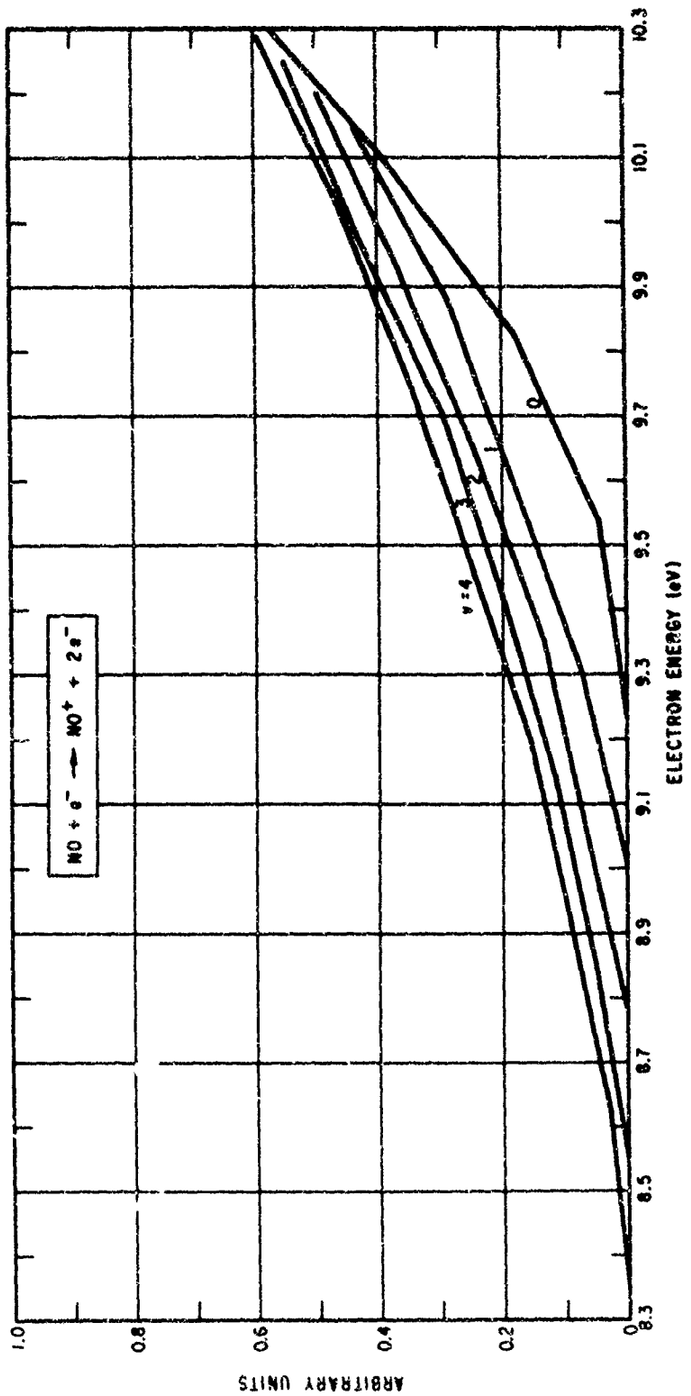


Fig. 23. Threshold Behavior of NO Ionization CS

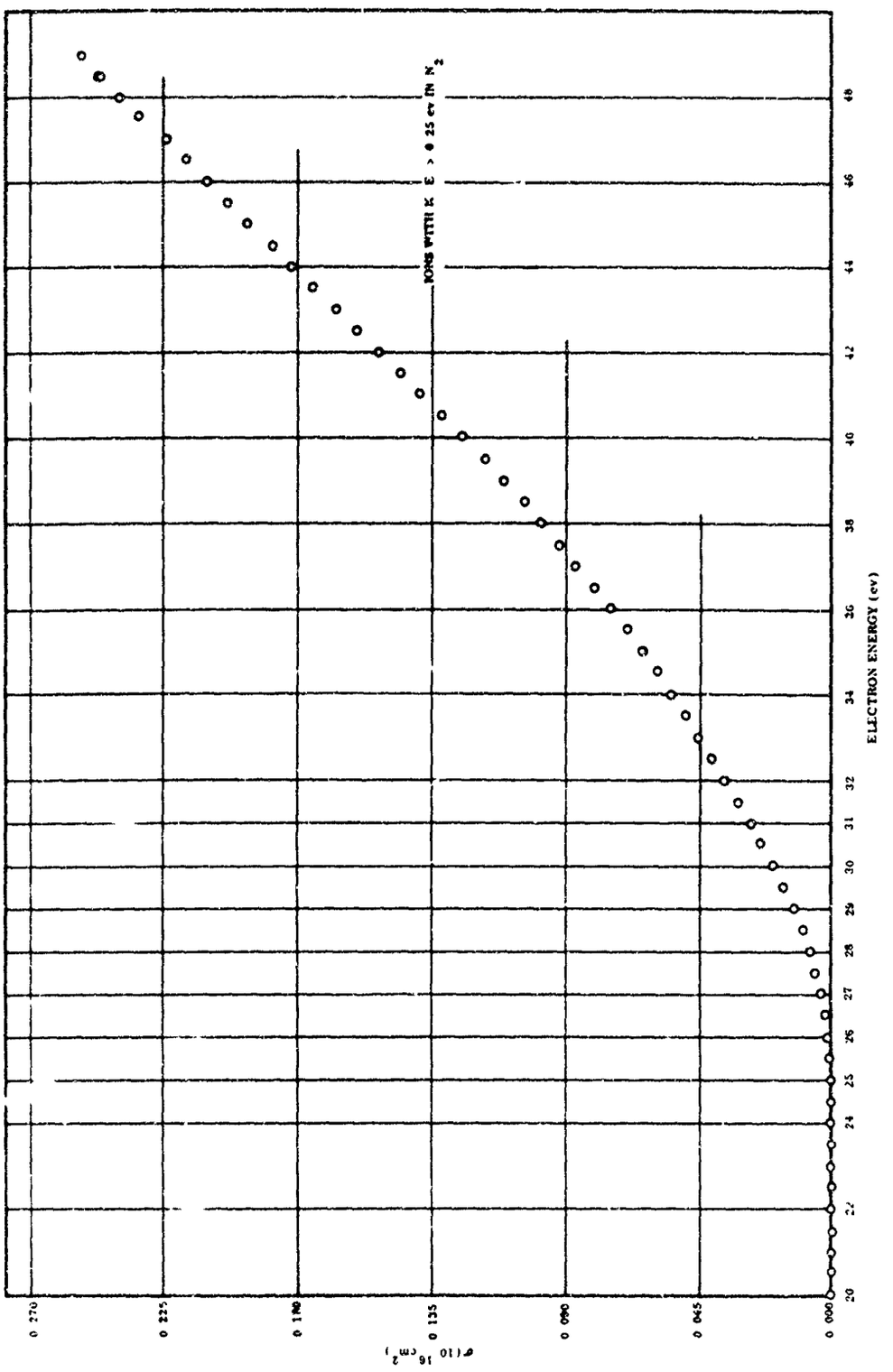


Fig. 24. Dissociative Ionization CS in $N_2$ (from Ref. 22)

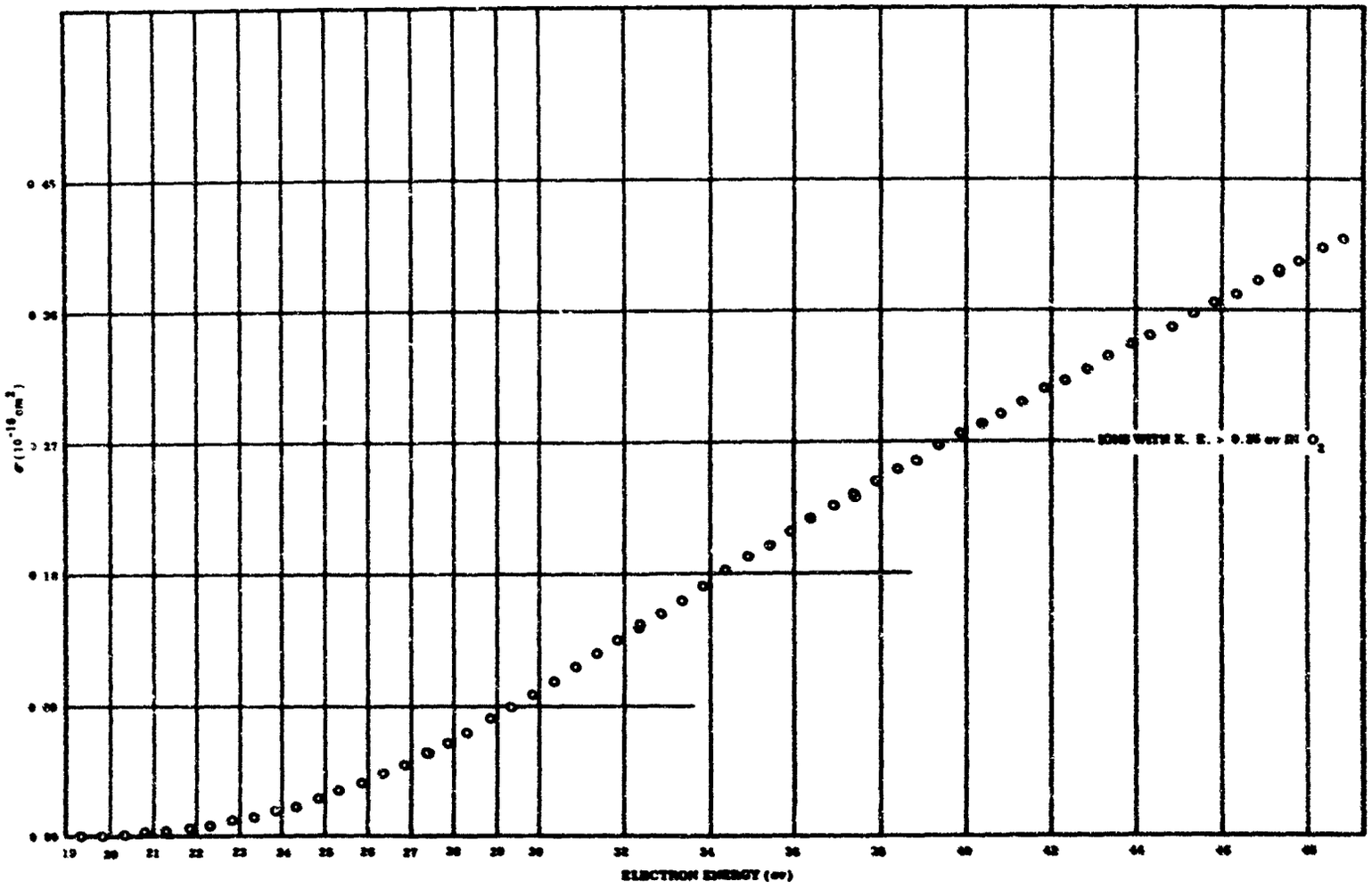


**Fig. 25. Dissociative Ionization CS in $O_2$ (from Ref. 22)**

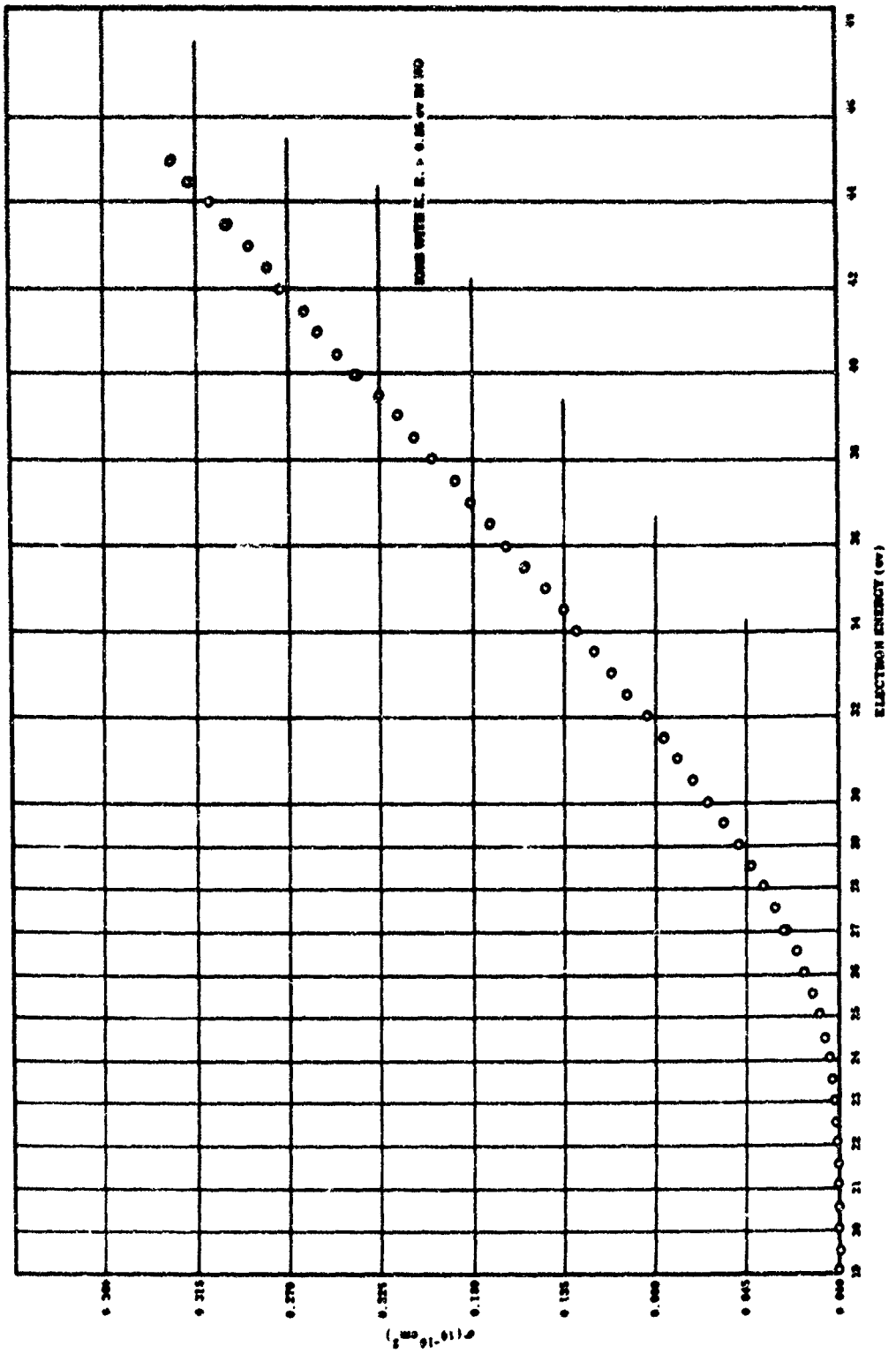

Fig. 26. Dissociative Ionization CS in NO (from Ref. 22)

## IX. RECOMBINATION OF ELECTRONS WITH IONS

Recombination in atomic ions is a radiative process and may be calculated from the photoionization CS by the detailed balancing relationship given in Eq. (10). For molecular ions the radiative process also exists but is much less important than the dissociative recombination process. Cross Sections for the radiative processes as have been calculated (Ref. 28) from Eq. (10) are presented in Figs. 27 and 28. These CS were calculated from an analytic representation of the photoionization CS above threshold as parabolic in the wavelength of the photon (examination of the data, Refs. 29 and 30, shows this to be a good representation) used in Eq. (10). This gives the recombination CS as

$$\sigma_R = 9.78 \times 10^{-7} \frac{(E + E_o)^2}{E} \frac{g_o}{g_+} \left[ \sigma_m - \delta \left( \frac{1}{E + E_o} - \frac{1}{E_m} \right) \right] \qquad (14)$$

where E is the electron energy in eV, $E_o$ the threshold energy in eV, $E_M$ is the energy in eV of the maximum of the parabola, $\sigma_M$ is the CS at $E_M$, $\delta$ is fit to the parabola, and $g_o$ and $g_+$ are the statistical weights (Appendix) of the atom and ion, respectively. This is for recombination into the ground state only.

Table 12 gives the constants for the analytical representation of the photoionization CS in units of $cm^2$ as a function of energy in eV. Table 12 values are obtained from visual estimates of theoretical (Ref. 29) or experimental (Ref. 30) curves so that the resultant CS are to be understood as being rough and not to be taken too seriously.

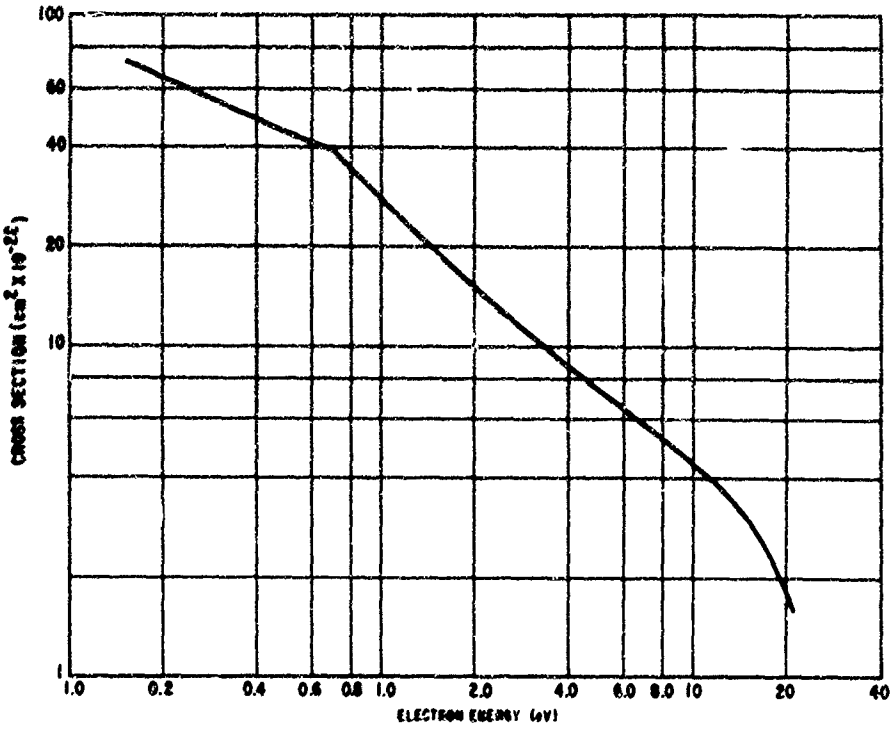


Fig. 27. Electron Radiative Attachment CS to $N_2^+$ (calculated from detailed balancing from photo ionization data)

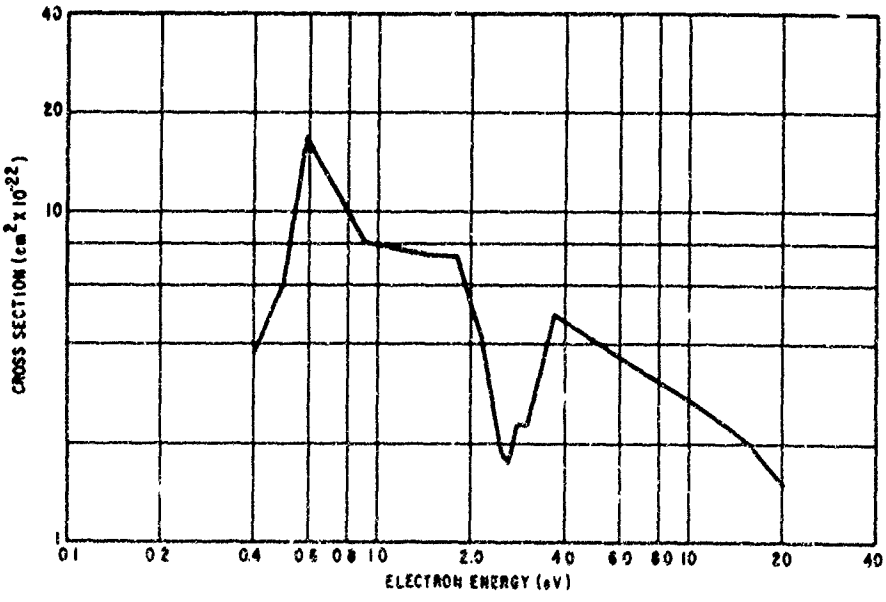


Fig 28. Electron Radiative Attachment CS to $O_2^+$

Table 12. Parameters for Eq. (14)

| Specie | $\sigma_M(10^{-18}cm^2)$ | $\delta(10^{-13}cm^2/eV)$ | $E_o$, eV | $E_M$, eV | Range of Validity, eV |
|---|---|---|---|---|---|
| $N^+$ | -- | -- | 14.48 | -- | Insufficient data |
| $O^+$ | 3.5 | $1.73 \times 10^{-3}$ | 13.55 | 20.7 | 0.2 - 2.0 |
| $A^+$ | 35 | 1.70 | 15.7 | 18.5 | 0.2 - 5.6 |
| $N_2^+$ | 21 | 4.11 | 15.6 | 17.2 | 0.2 - 3.4 |
| $O_2^+$ | 13.0 | 2.29 | 12.1 | 13.9 | 0.4 - 3.4 |
| $NO^+$ | -- | -- | -- | -- | Insufficient data |

The threshold analysis of Geltman (Ref. 19) indicates the low energy behavior of the radiative recombination to be

$$\sigma_R \sim \frac{(E + E_o)^3}{1 - \exp(-2\pi/E)} \cdot \frac{1}{E} \qquad (15)$$

$$\sim \frac{(E + E_o)^3}{E}, \quad E_{small}$$

where E is electron energy, and $E_o$ is the photoionization threshold. Note that $E_o^2/E$ must be of the order of $10^6$ eV in order that $\sigma_R$ be equal to the threshold photoionization CS, which will occur for $E > 10^{-4}$ eV. The low energy behavior for recombination rates will then be as $E^{-1/2}$.

Measured reaction rates for dissociative recombination indicate that there are very large CS ($10^{-14}$ - $10^{-13}$ $cm^2$) for this process although they have not been directly measured. Certain properties of the CS can be inferred from the limited reaction rate data and crude theoretical estimates.

These are that the CS are large at low energy and decrease rapidly with increasing energy.

Of significance are (1) the experimental results of W. P. Thompson (Aerospace Corporation, Aerodynamics and Propulsion Research Laboratory) that indicate the reaction rate for $NO^+$ dissociative recombination is an order of magnitude larger than for $N_2^+$ and $O_2^+$ at room temperature and (2) the comment by Dalgarno (Ref. 14) that the rate for $N_2$ should be greater than for $O_2^+$ or $NO^+$. However, an examination of the potential energy diagrams (Ref. 1) for $NO^+$ and NO shows a substantial overlap of $X(NO^+)^1\Sigma^+$ and the repulsive $(NO)^2\Sigma^+$ states, which decays to $N(^4S) + O(^3P)$ with no electron rearrangement. In $N_2^+$ and $O_2^+$, the only available repulsive states require a spin change in the ion in order to form; thus, they will proceed as a second order process.

Radiative recombination of electrons with atomic and molecular ions is characterized by CS that are largest at low electron energies and on the order of $10^{-21}$ $cm^2$. The effect of gas temperature is difficult to estimate; however, it may be safely assumed that there is no pronounced amplification of the CS. Experimental CS are unknown directly but may be inferred from photoionization and detailed balancing. Dissociative recombination is characterized by CS on the order of $10^{-14}$ to $10^{-13}$ $cm^2$, as inferred from reaction rates. However, there are no direct measurements of CS for this process.

## X. ELASTIC CROSS SECTIONS

Elastic scattering CS for electrons on neutral atoms and molecules have been well established by electron beam techniques for energies above 2 to 3 eV (Refs. 31 and 32) and even down to 0.6 eV for the inert gases (Ref. 33). For lower electron energies, one must rely on the swarm experiment approach (Refs. 4 and 34).

For energies above a few eV, the CS for $N_2$, NO, and $O_2$ appear to have the relative magnitude and behavior one would expect because they are neighbors on the molecular scale. Near 2 eV, $N_2$ exhibits the metastable state resonance and below that, the effect of the induced polarization as predicted by theory (Ref. 35). For NO, the effect of the permanent dipole, as seen for CO and other polar molecules (Ref. 34) dominates in the low energy range, and we may infer a CS in that range from experiment at higher energies continued to lower energies by a combination of Altshuler's (Ref. 36) and O'Malley's (Ref. 37) theories. Although the low energy CS for N and O have been calculated (Refs. 38 and 39), the CS for $N_2$ and $O_2$ will have to be continued to low energy in a manner consistent with the theory (Ref. 37).

For a neutral, polarizable scatterer at low energy, the elastic CS can be represented by

$$\sigma(E) = \frac{3.52}{10^{16}}\left[A^2 + \frac{2\pi}{3}\alpha A\left(\frac{E}{13.6}\right)^{1/2} + \frac{4}{3}\alpha A^2\,\frac{E}{13.6}\log\left(\frac{E}{13.6}\right) + \sigma'(E)\right] \quad (16)$$

where A is the scattering length in atomic units, $\alpha$ is the static polarizability in atomic units (length = 0.53Å), E is in eV, and $\sigma$ is in $cm^2$. Examples of $\alpha$ and A are given in Table 13 for N, O, and A.

Table 13. Polarizabilities and Scattering Lengths for N, O, and A

| Specie | $\alpha(a_o^3)$ | $A(a_o)$ |
|---|---|---|
| N | 7.65 | 0.333 |
| O | 5.20 | 0.300 |
| A | 11.0 | -1.70 |

Equation (16) cannot be applied to homonuclear diatomic molecules because they possess permanent quadrupole moments that dominate the effect of the induced polarization. As may be seen from Figs. 29 and 32, the CS for $N_2$ has the same functional dependence on $(E)^{1/2}$, for $(E)^{1/2}$, small, as does Eq. (16); however, the coefficients of the functions of $(E)^{1/2}$ are not predictable in terms of the polarizability and quadrupole moment.

For a heteronuclear diatomic molecule that has a permanent dipole moment, such as NO, the low energy CS behaves as $E^{-1}$ when E is large enough that the electron's DeBroglie wavelength is less than the interparticle distance. Below this energy, the electron is experiencing the fields of several atoms simultaneously; thus, one cannot speak of a single scattering. This lower limit of energy for the wavelength twice the interparticle distance is given by $E(eV) = 2.76 \times 10^{-16} n_o^{2/3}$, where $n_o$ is the particle density. For NO, the elastic CS will be essentially constant from 0.1 to 20 eV, but below 0.1 eV the dipole behavior will take effect, i.e., $\sigma \sim E^{-1}$.

Elastic CS for N, O, A, $N_2$, NO, and $O_2$ are given in Figs. 29 through 33. Also, for $O_2$, see Fig. 2(b) for Phelp's estimates of the elastic CS from swarm experiment data.

An elastic CS summary is presented in Table 14.

Table 14. Elastic CS Summary

| Specie | CS | Effect of Gas Temperature | Range of Validity, eV | Remarks |
|---|---|---|---|---|
| N | Eq. (16), Fig. 29 | No appreciable effect for temperatures of reentry interests | $E_{n_o}$ - 20 | Reliable estimate |
| O | Eq. (16), Fig. 30 | | $E_{n_o}$ - 20 | Reliable estimate |
| A | Eq (16), Fig. 31 | | $E_{n_o}$ - 20 | Reliable estimate[a] |
| $N_2$ | Fig. 32 | | $E_{n_o}$ - 20 | Reliable Estimate |
| $O_2$ | Fig. 33 | | $E_{n_o}$ - 20 | ±20%, 0.2 - 20 eV; below 0.2 eV reasonable |
| NO | Fig. 33 | | $E_{n_o}$ - 20 | Rough estimate, but reasonable for energy > 0.1 eV |

[a]Possible gas temperature effect in the energy range of the metastable ion formation in $N_2$. See Section IV.

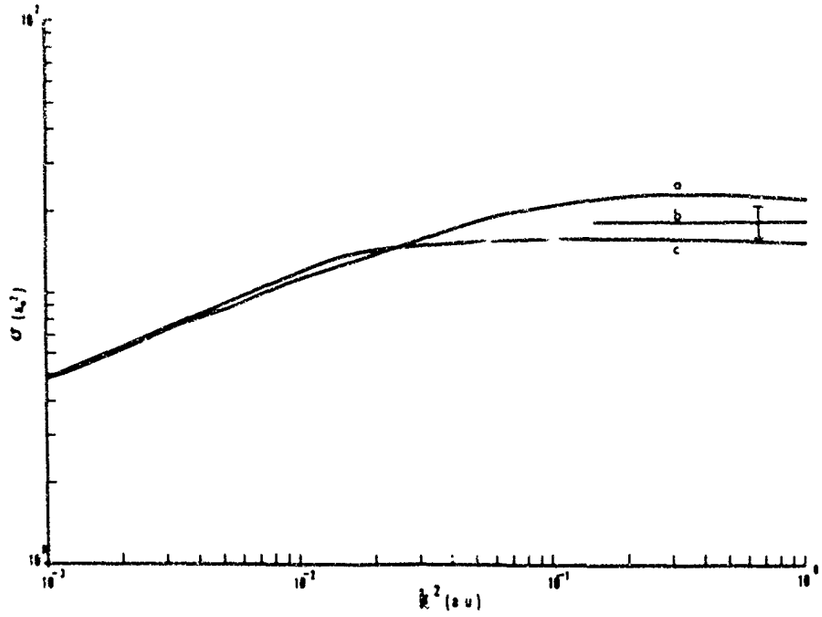


Fig. 29. Elastic CS for Nitrogen (from Ref 39)

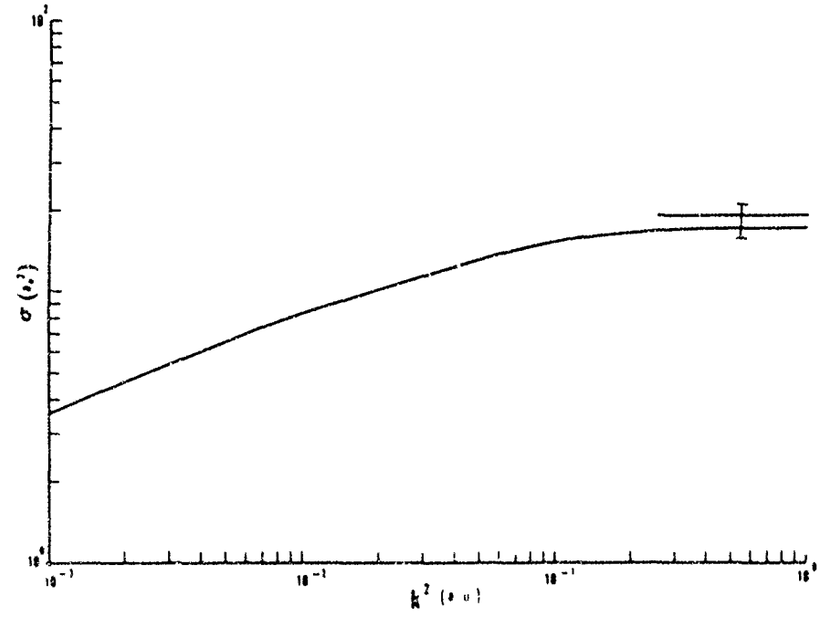

Fig. 30. Elastic CS for Oxygen (from Ref. 39)

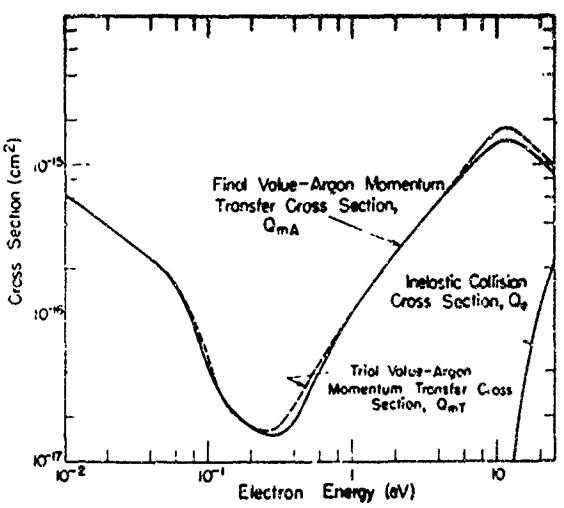


Fig. 31. Momentum Transfer and Inelastic Collision CS for Electrons in Argon as a Function of Electron Energy in eV (from Ref. 40)

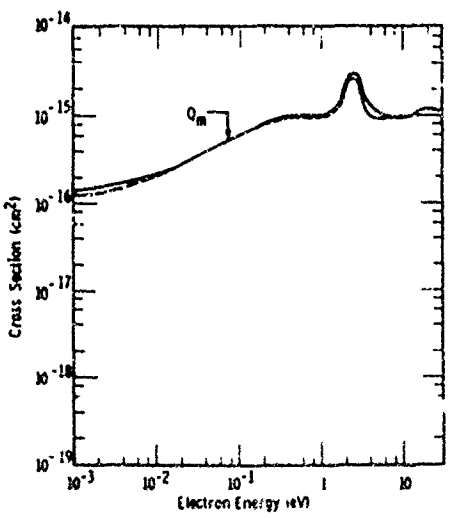


Fig. 32. Momentum Transfer $Q_m$ and Inelastic Collision CS for Electrons in $N_2$ (from Ref. 4)

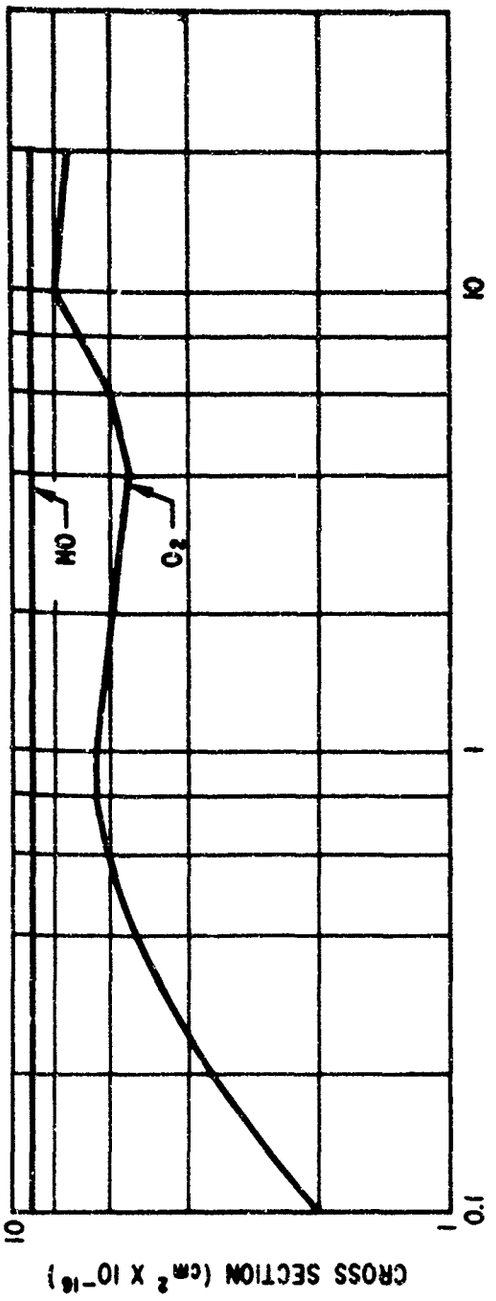


Fig. 33. Elastic CS for $O_2$ and NO

## XI. ELECTRON IMPACT DISSOCIATION

The best identification of an electron impact dissociation (discussed in Section V) is the $O_2\left(X^3\Sigma_g^-\right) \rightarrow O(^3P) + O(^3P)$ process shown in Fig. 5 to occur effectively between 4.5 and 8 eV. The process appears to proceed as a highly resonant type CS as depicted by Eq. (8). It is believed that the effect to temperature on the dissociative process will be essentially the same as that proposed for the resonant dissociative attachment process (Ref. 22) in that the resonant peak is made broader and the peak goes down as one over the partition function.

Direct dissociation of $N_2\left(X^1\Sigma_g^+\right) \rightarrow N(^4S) + N(^4S)$ would occur above 10 eV electron energy and would appear to be quite small in magnitude due to a small overlap in the bound and free nuclear wave functions. For higher state dissociation in $N_2$, it is difficult to comment because of the complexity of states in this energy range (Ref. 1).

For $NO(X^2\pi) \rightarrow N(^4S) + O(^3P)$ dissociation, the process probably follows a transition to a repulsive $^2\Sigma^+$ state beginning at 8.5 eV and dissociating from there. The peak of the CS is probably a characteristic $10^{-18}$ $cm^2$ and the upper energy cutoff is probably about 9 eV, leading to a very sharp resonance.

Cross sections for dissociation in $N_2$ and NO are not known. Two dissociation peaks at 6.1 and 8.2 eV may be identified and analytically represented for $O_2$ using Fig. 5 and Eq. (8). Since $O_2$ is the first molecule to dissociate in air these two CS are probably quite important.

# APPENDIX

## STATES OF ATOMS AND MOLECULES IN A GAS

The electronic states of atoms are classified as multiplets according to the angular momentum (discrete) and the multiplicity of the state. The customary symbol for an atomic state is $^{M}A$, where M is the multiplicity and A depends on the angular momentum. Traditionally, the letters S, D, F, and in alphabetic progression (excluding J) thereafter are used for angular momentum values 0, 1, 2, 3 · · ·, respectively. For a given number of electrons in an atom, more than one may arise multiplet; e. g., oxygen with three, $^{3}P$, $^{1}D$, and $^{1}S$. There is a rule that the multiplet with the highest multiplicity and highest angular momentum will lie lowest in energy and thus be the ground state. For oxygen this is $^{3}P$. The energies of these multiplets are measured negatively downward from the first ionization potential; thus the magnitude of the $^{3}P$ energy, $E(^{3}P)$, will be greater than the $^{1}D$, but $E(^{1}D)$ minus $E(^{3}P)$ will be positive, and $^{1}D$ will be said to lie above $^{3}P$ (in energy).

Diatomic molecules have two additional degrees of freedom, vibrational and rotational motion. These motions are usually considered to be independent of each other and give rise to the classification of particular energy states in terms of electronic vibrational, and rotational states. The electronic states, analogous to the atomic states, are called multiplets, but are designated $\Sigma$, $\pi$, $\Delta$, $\Phi$, · · ·, rather than S, P, D, F, · · · . The vibrational states are numbered v = 0, 1, 2, · · · , as are the rotational states J = 0, 1, 2, · · · . There are expressions for the energies of these motions, referenced to zero energy, because the total energy of the combined state will be the sum of the individual motions, the electronic (negative), the vibrational (positive), and rotational (positive). For a diatomic molecule, the multiplet energy is referenced to the dissociation energy and is usually on the order of several eV. The vibrational energy (0. 1 eV) is then superimposed on the

electronic energy, and the rotational energy (0.001 eV) is superimposed on the vibrational energy. The vibrational energy is given by

$$E_v = \omega_e\left(v + \frac{1}{2}\right) - \omega_e X_e\left(v + \frac{1}{2}\right)^2 \qquad \text{(A-1)}$$

and the rotational energy is given by

$$E_J = J(J + 1)B \qquad \text{(A-2)}$$

where $\omega_e$, $\omega_e X_e$, and B are given for various molecules in Ref. 7. The degeneracy of the Jth rotational level is (2J + 1). Then, the energy of a given state ($^3\Sigma vJ$) will be

$$E(^3\Sigma vJ) = E_X + E_v^X + E_J^X \quad , \quad X = {}^3\Sigma \qquad \text{(A-3)}$$

The ground state of a diatomic molecule is the lowest energy multiplet with v = J = 0. As implied before, the magnitudes of $E_x$, $\omega_e$, $\omega_e X_e$, and B are several, 0.1, 0.001 and 0.0001 eV respectively.

In a gas comprised of many atoms in thermal equilibrium the probability that a particular atom will be in a given state with degeneracy $g_n$ with an energy $\Delta E_n$ above the ground state is

$$P_n = \frac{g_n \exp(-\Delta E_n / kT)}{P(T)} \qquad \text{(A-4)}$$

where the partition function P is

$$P(T) = \sum_{n \geq 0} g_n \exp - \frac{\Delta E_n}{kT} \qquad \text{(A-5)}$$

T is the gas temperature, and k is Boltzmann's constant. For oxygen atoms with the three lowest states $^3P$, $^1D$, and $^1S$, one would have $\Delta E_o = 0$, $\Delta E_1 = E(^1D) - E(^3P)$, and $\Delta E_2 = E(^1S) - E(^3P)$. The degeneracy is the multiplicity times $(2L + 1)$, where L is the angular momentum of the state in units of 0, 1, 2, · · · , for S, P, $D_1$ · · · , or $\Sigma$, $\pi$, $\Delta_1$ · · · . Then, for oxygen, the partition function proceeds as

$$P(T) = 9 + 5 \exp - \frac{\Delta E_1}{kT} + \exp - \frac{\Delta E_2}{kT} + \cdots \qquad (A\text{-}6)$$

In oxygen, $\Delta E_1 \simeq 2$ eV and $\Delta E_2 \simeq 4$ eV; therefore for gas temperatures of 6000°K, it is clear that the ground state is by far the most probable.

For diatomic molecules where the separation of electronic, vibrational, and rotational motion is assumed, the contribution to the partition function from all the states superimposed on the electronic state is given by $g_n \exp(-\Delta E_n/kT)$ for the electronic level times the sum of the like terms for the vibrational and rotational states. That is

$$P(T) = \sum_{n \geq 0} g_n \exp - \frac{\Delta E_n}{kT} \left( \sum_{v \geq 0} \exp - \frac{E_v^n}{kT} \right) \left[ \sum_{J \geq 0} (2J + 1) \exp - \frac{\Delta E_J^n}{kT} \right] \qquad (A\text{-}7)$$

With the aid of the partition function, temperature-dependent or gas-state-dependent CS may be written. The $p_n$ of Eq. (A-4) gives the probability that a given particle in the gas will be in the nth state; thus, the CS for a particular process, such as ionization, will be the sum over the products of the probability of being in the nth state times the CS for ionization from the nth state. For ionization of oxygen by an electron of energy E, there would result

$$\sigma_i(E, T) = \frac{1}{P(T)} \left[ 9\sigma_i(^3P, E) + 5\sigma_i(^1D, E) \exp - \frac{\Delta E_1}{kT} + \sigma_i(^1S, E) \exp - \frac{\Delta E_2}{kT} + \cdots \right] \qquad (A\text{-}8)$$

where $\Delta E_1$ and $\Delta E_2$ are as in Eq. (A-6), $\sigma_i(^3P, E)$ is the ionization CS for ionization from the $^3P$ state by an electron of energy E, and similarly for $\sigma_i(^1D, E)$ and $\sigma_i(^1S, E)$.

## REFERENCES


1. F. R. Gilmore, "Potential Energy Curves for $N_2$, NO, $O_2$, and Corresponding Ions," Rand Corporation Memo, RM-4034-PR, (June 1964).

2. E. Gerjuoy and S. Stein, "Rotational Excitation by Slow Electrons," Phys. Rev. 97, 1671 (1955).

3. L. S. Frost and A. V. Phelps, "Rotational Excitation and Momentum Transfer Cross Sections for Electrons in $H_2$ and $N_2$ from Transport Coefficients," Phys. Rev. 127, 1621 (1962).

4. A. G. Englehart, A. V. Phelps, and C. G. Risk, "Determination of Momentum Transfer and Inelastic Collision Cross Sections for Electrons in Nitrogen using Transport Coefficients," Phys. Rev. 135, A1566 (1964).

5. R. C. Mjolsness and D. H. Sampson, "Distorted-Wave Calculation of Rotational Excitation of $N_2$ by Slow Electrons," Phys. Rev. Letters 13, 812 (1964).

6. K. Takayanagi and S. Geltman, "Excitation of Molecular Rotation by Slow Electrons," Phys. Rev. 138, A1003 (1965).

7. G. Herzberg, Spectra of Diatomic Molecules, 2nd ed., D. Van Nostrand Company, Inc., New York (1950),p. 125.

8. G. J. Schulz, "Vibrational Excitation of Nitrogen by Electron Impact," Phys. Rev. 125, 229 (1962).

9. A. V. Phelps, "Studies and Experimental Work on Atomic Collision Processes Occurring in Atmospheric Gases," Westinghouse Research Laboratories Report, AFWL TR-64-178.

10. J. C. Y. Chen, "Theory of Subexcitation Electron Scattering by Molecules," Part I and II, J. Chem. Phys. 40, 3507 (1964); erratum, J. Chem. Phys. 41, 3263 (1964).

11. G. J. Schultz, "Vibrational Excitation of $N_2$, CO, and $H_2$ by Electron Impact," Phys. Rev. 135, A988 (1964).

12. G. J. Schulz and J. T. Dowell, "Excitation of Vibrational and Electronic Levels in $O_2$ by Electron Impact," Phys. Rev. 128, 174 (1962).

13. A. Dalgarno, "Charged Particles in the Upper Atmosphere," Ann. de Phys. 17(1), 16 (1961).

14. L. M. Branscomb, D. S. Burch, S. J. Smith, and S. Geltman, "Photodetachment Cross Section and Electron Affinity of Atomic Oxygen," Phys. Rev. 111, 504 (1958).

15. J. W. Cooper and J. B. Martin, "Electron Photodetachment from Ions and Elastic Cross Sections for O, C, Cl, and F," Phys. Rev. 126, 1482 (1962).

16. D. S. Burch, S. J. Smith, and L. M. Branscomb, "Photodetachment of $O_2^-$," Phys. Rev. 112, 171 (1958).

17. H. T. Jackson, Jr. and W. R. Garrett, "Theoretical Photodetachment Cross Section for the Negative Atomic Oxygen Ion," Univ. of Ala. Res. Inst. Report No. 32 (Preliminary).

18. L. M. Branscomb, "Photodetachment" Atomic and Molecular Processes," ed. D. R. Bates, Academic Press, New York (1962).

19. S. Geltman, "Theory of Threshold Energy Dependence of Photodetachment of Diatomic Molecular Negative Ions," Phys. Rev. 112, 176 (1958).

20. D. Rapp and D. D. Briglia, "Total Cross Sections for Negative Ion Formation in Gases by Electron Impact," J. Chem. Phys. 43, 1480 (1965).

21. E. E. Muschlitz, Jr., "Elastic and Inelastic Collisions of Low Energy Negative Ions in Gases," Proc. Intl. Conf. Ionization Phenomena Gases, 4th, Uppsala, 1959, 1, 52 (1960).

22. D. Rapp, T. E. Sharp, and D. D. Briglia, "On the Theoretical Interpretation of Resonance Dissociative Attachment Cross Sections," Lockheed Missiles and Space Company Report, LMSC 6-74-64-45 (1964).

23. A. C. Smith, E. Caplinger, R. H. Neynaber, E. W. Rothe, and S. M. Trujillo, "Electron Impact Ionization of Atomic Nitrogen," Phys. Rev. 127, 1647 (1962).

24. E. W. Rothe, L. L. Marino, R. H. Neynaber, and S. M. Trujillo, "Electron Impact Ionization of Atomic Hydrogen and Atomic Oxygen," Phys. Rev. 125, 582 (1962).

25. P. Englander-Golden and D. Rapp, "Total Cross Sections for Ionization of Atoms and Molecules by Electron Impact," J. Chem Phys. 43, 1464 (1965).

26. C. E. Brion, "Ionization of Oxygen by 'Monoenergetic' Electrons," J. Chem. Phys. 40, 2995 (1964).

27. J. W. McGowan, E. M. Clarke, H. P. Hanson, and R. F. Stebbings, "Electron- and Photon-Impact Ionization of $O_2$," Phys. Rev. Letters 13, 620 (1964).

28. A. Dalgarno, R. J. W. Henery, and A. L. Stewart, "The Photo-ionization of Atomic Oxygen," Planetary Space Sci. 12, 235 (1964).

29. A. Dalgarno, "The Photoionization of Atomic Nitrogen and Oxygen," J. Atmospheric Terrest. Phys. 18, 335 (1960).

30. N. Wainfain, W. C. Walker, and G. L. Weissler, "Photoionization Efficiencies and Cross Sections in $O_2$, $N_2$, $CO_2$, A, $H_2O$, $H_2$ and $CH_4$," Phys. Rev. 99, 542 (1955).

31. R. H. Neynaber, L. L. Marino, E. W. Rothe, and S. M. Trujillo, "Low-Energy Electron Scattering From Atomic Oxygen," Phys. Rev. 123, 148 (1961).

32. R. H. Neynaber, L. L. Marino, E. W. Rothe, and S. M. Trujillo, "Low-Energy Electron Scattering from Atomic Nitrogen," Phys. Rev. 129, 2069 (1963).

33. C. Ramsauer and R. Kollath, Ann. Physik 3, 536 (1929); 12, 529 (1932); and 12, 837 (1932).

34. J. L. Pack, R. E. Voshall, and A. V. Phelps, "Drift Velocities of Slow Electrons in Krypton, Xenon, Deuterium, Carbon Monoxide, Carbon Dioxide, Water Vapor, Nitrous Oxide and Ammonia," Phys. Rev. 127, 2084 (1962).

35. T. F. O'Malley, L. Spruch, and L. Rosenberg, "Modification of Effective-Range Theory in the Presence of a Long-Range ($r^{-4}$) Potential," J. Math. Phys. 2, 491 (1961).

36. S. Aultshuler, "Theory of Low-Energy Electron Scattering by Polar Molecules," Phys. Rev. 107, 114 (1957).

37. T. F. O'Malley, "Low-Energy Expansion of the Scattering Amplitude for Long-Range Quadrupole Potentials," Phys. Rev. 134, A1188 (1964).

38. A. Temkin, "Polarization and Exchange Effects in the Scattering of Electrons from Atoms with Application to Oxygen," Phys. Rev. 107, 1004 (1957).

39. C. J. Lenander, "Low Energy Elastic Scattering from Atoms and Molecules: A Model," Bull. Am. Phys. Soc. 10, 185 (1965). Phys. Rev. 142, 1 (1966).

40. A. G. Engelhardt and A. V. Phelps, Phys. Rev. 133, A375 (1964).

41. J. C. Y. Chen, "Vibrational Excitation of Molecules by Slow Electron Impact, Atomic Collision Processes, ed. M. R. C. McDowell, John Wiley and Sons, Inc., New York (1964), p. 437.

26. C. E. Brion, "Ionization of Oxygen by 'Monoenergetic' Electrons," J. Chem. Phys. 40, 2995 (1964).

27. J. W. McGowan, E. M. Clarke, H. P. Hanson, and R. F. Stebbings, "Electron- and Photon-Impact Ionization of $O_2$," Phys. Rev. Letters 13, 620 (1964).

28. A. Dalgarno, R. J. W. Henery, and A. L. Stewart, "The Photoionization of Atomic Oxygen," Planetary Space Sci. 12, 235 (1964).

29. A. Dalgarno, "The Photoionization of Atomic Nitrogen and Oxygen," J. Atmospheric Terrest. Phys. 18, 335 (1960).

30. N. Wainfain, W. C. Walker, and G. . . Weissler, "Photoionization Efficiencies and Cross Sections in $O_2$, $N_2$, $CO_2$, A, $H_2O$, $H_2$ and $CH_4$," Phys. Rev. 99, 542 (1955).

31. R. H. Neynaber, L. L. Marino, E. W. Rothe, and S. M. Trujillo, "Low-Energy Electron Scattering From Atomic Oxygen," Phys. Rev. 123, 148 (1961).

32. R. H. Neynaber, L. L. Marino, E. W. Rothe, and S. M. Trujillo, "Low-Energy Electron Scattering from Atomic Nitrogen," Phys. Rev. 129, 2069 (1963).

33. C. Ramsauer and R. Kollath, Ann. Physik 3, 536 (1929), 12 529 (1932); and 12, 837 (1932).

34. J. L. Pack, R. E. Voshall, and A. V. Phelps, "Drift Velocities of Slow Electrons in Krypton, Xenon, Deuterium, Carbon Monoxide, Carbon Dioxide, Water Vapor, Nitrous Oxide and Ammonia," Phys. Rev. 127, 2084 (1962).

35. T. F. O'Malley, L. Spruch, and L. Rosenberg, "Modification of Effective-Range Theory in the Presence of a Long-Range ($r^{-4}$) Potential," J. Math. Phys. 2, 491 (1961).

36. S. Aultshuler, "Theory of Low-Energy Electron Scattering by Polar Molecules," Phys. Rev. 107, 114 (1957).

37. T. F. O'Malley, "Low-Energy Expansion of the Scattering Amplitude for Long-Range Quadrupole Potentials," Phys. Rev. 134, A1188 (1964).

38. A. Temkin, "Polarization and Exchange Effects in the Scattering of Electrons from Atoms with Application to Oxygen," Phys. Rev. 107, 1004 (1957).

39. C. J. Lenander, "Low Energy Elastic Scattering from Atoms and Molecules: A Model," Bull. Am. Phys. Soc. 10, 185 (1965); Phys. Rev. 142, 1 (1966).

40. A. G. Engelhardt and A. V. Phelps, Phys. Rev. 133, A375 (1964).

41. J. C. Y. Chen, "Vibrational Excitation of Molecules by Slow Electron Impact, Atomic Collision Processes, ed. M. R. C. McDowell, John Wiley and Sons, Inc., New York (1964), p. 437.

UNCLASSIFIED
Security Classification

**DOCUMENT CONTROL DATA · R&D**

*(Security classification of title, body of abstract and indexing annotation must be entered when the overall report is classified)*

| 1 ORIGINATING ACTIVITY (Corporate author) | 2a REPORT SECURITY CLASSIFICATION |
|---|---|
| Aerospace Corporation<br>El Segundo, California | Unclassified |
| | 2b GROUP |

3 REPORT TITLE

ELECTRON COLLISION CROSS SECTIONS IN AIR AND THE EFFECTS OF ELEVATED GAS TEMPERATURES

4 DESCRIPTIVE NOTES (Type of report and inclusive dates)

5 AUTHOR(S) (Last name, first name, initial)

Lenander, Carl J.

| 6 REPORT DATE | 7a. TOTAL NO. OF PAGES | 7b. NO. OF REFS |
|---|---|---|
| May 1966 | 78 | 41 |

| 8a CONTRACT OR GRANT NO. | 9a. ORIGINATOR'S REPORT NUMBER(S) |
|---|---|
| AF 04(695)-669 | TR-669(6240-20)-7 |
| b. PROJECT NO. | |
| c | 9b OTHER REPORT NO(S) (Any other numbers that may be assigned this report) |
| d | SSD-TR-66-153 |

10 AVAILABILITY/LIMITATION NOTICES

This document is subject to special export controls, and each transmittal to foreign governments or foreign nationals may be made only with prior approval of SSD (SSTRT).

| 11 SUPPLEMENTARY NOTES | 12 SPONSORING MILITARY ACTIVITY |
|---|---|
| | Space Systems Division<br>Air Force Systems Command<br>Los Angeles, California |

13 ABSTRACT

Elastic and inelastic electron scattering cross sections in air or its constituent gases are normally studied at low gas temperatures; therefore the initial state of the scatterer is the ground state. However, in the study of transport phenomena in gases, such as the propagation of intense electromagnetic waves through a reentry flow field where the gas temperature may easily reach a value on the order of 6,000°K and the electron temperature may be many times that value, it is necessary to include the effect of the scatterers being distributed in excited states as well as in the ground state. For the temperatures of interest, the states populated will be rotational and vibrational, with virtually no effect from excited electronic levels because they lie too high in energy above the ground state. The species considered are N, O, A, $N_2$, $O_2$, and NO and some of their ions. This report is intended as a catalogue of the best available cross sections for the various processes and is presented in a manner to be useful as an aid in transport phenomena calculations.

DD FORM 1473

UNCLASSIFIED
Security Classification

UNCLASSIFIED
Security Classification

| 14. KEY WORDS |
| --- |
| Electron Scattering in Air<br>Temperature Effects in Air<br>Cross Sections |
| Abstract (Continued) |

UNCLASSIFIED
Security Classification